4-20-2024

Biomimetic and bio-derived composite phase change materials for thermal energy storage applications: A thorough analysis and future research directions

Md Shahriar Mohtasim

Barun K. Das
Edith Cowan University

Review article

Biomimetic and bio-derived composite Phase Change Materials for Thermal Energy Storage applications: A thorough analysis and future research directions

Md. Shahriar Mohtasim [a], Barun K. Das [b],*

[a] Department of Mechanical Engineering, Rajshahi University of Engineering and Technology, Rajshahi 6204, Bangladesh
[b] School of Engineering, Edith Cowan University, Joondalup, WA 6027, Australia

ABSTRACT

Phase change heat storage has gained a lot of interest lately due to its high energy storage density. However, during the phase shift process, Phase Change Materials (PCMs) experience issues such as low thermal conductivity, stability, leaking, and low energy-storing capacity. Materials that mimic or derive from nature can effectively offset the shortcomings attributed. This work presents a methodical overview of the synthesis, thermo-physical properties, comparison and Thermal Energy Storage (TES) applications of bio-derived and biomimetic composite PCMs (BD/BM-CPCMs). Several studies have observed increase in thermal conductivity up to 950–1250 % for BD/BM-CPCMs, as well as great thermal stability with no matrix leakage at an average temperature of 150–250 °C. These types of composites have a relative enthalpy efficiency of up to 98.1 % and can endure 200–1000 heating-cooling cycles on average. Additionally, enviro-economic aspects, numerical approaches to heat transfer during phase change and multivariate and multi-objective optimizations from a technical, financial and environmental standpoint using machine learning techniques with underlying scopes of BD/BM-CPCM are presented. It is necessary to fabricate adaptable BD/BM-CPCM for multifunctional energy harvesting and storage in future. With regard to the advancement in substance functionalism, it is necessary to show and research the use of bio-derived composite with innovative effects like versatility, light to thermal conversion, electro-thermal conversion, and anti-bacterial qualities in real-world systems.

1. Introduction

The usage of fossil fuels has rapidly expanded due to the quick growth of society and an upsurge in population. To avoid doing irreparable harm to our ecosystem, solar energy is a viable substitute for scarce fossil fuels [1,2]. Solar energy is intermittent and discontinuous, which results in low energy efficiency. Advanced energy storage technology development is essential to increase its integration and utilization efficiency [3]. Thermal energy storage (TES) based on Phase Change Materials (PCMs) has received the most attention among the many methods of energy storing. PCM is used more effectively in solar energy applications having benefits of elevated latent heat and a practically constant phase-change temperature. According to their chemical structure, the PCMs utilized for TES are usually grouped into four categories: organic, inorganic, inorganic-organic eutectic, and composite PCMs [4,5]. Mehling and Cabeza provided a different, more precise classification in 2007 [6], which is depicted in Fig. 1 and emphasizes the temperatures of the phase evolution and the latent heat of PCMs.

The use of TES technology improves the reliability of energy supply. Moreover, the TES technology guarantees dependability and economic viability over the long run. By lowering energy wastage and ultimately resulting in pollution management, the establishment of reliable TES is a significant step towards optimal energy usage. The energy is made more accessible by the TES devices by transferring heat through the working medium. The sensible heat energy storage (SHES) [7–10], latent heat energy storage (LHES) [11–13], thermo-chemical energy storage (TCES) [14,15] and sorption heat storage [16] are generic categories for TES depending on the type of heat transfer. The four main TES systems can be further divided into subcategories depending on a number of variables as shown in Fig. 2. Materials with excellent thermal conductivity, stability at high-temperature, volume changes slightly during heat storage, cost effective, and high resilience are included in SHES under the heat storage type TES system. The most popular liquid and solid

---

Nomenclature

C_p	Specific heat (J/kg.K)	LA-SA	Lauric-Stearic acid
g	Gravity (m/s^2)	ss-PCMs	shape-stable Phase Change Materials
h	Enthalpy (kJ)	RGO	Reduced Graphene Oxide
k	Thermal conductivity (W/m.K)	TES	Thermal Energy Storage
l	Length (m)	PU/WP	Polyurethane/Wood Powder
p	Pressure (kg/s^2.m)	BSiC	Bamboo-derived Silicon carbide
r	Radius (m)	PEG	Polyethylene Glycol
t	Time (s)	TiN	Titanium nitride
u, v	X, Y-component of velocity (m/s)	EG	Expanded Graphite
x, y, z	Cartesian coordinates (m)	CNF	Cellulose Nanofibers
w	Dimensionless geometric parameter	Sw	spider web
T	Temperature (K, °C)	LHTES	Latent Heat Thermal Energy Storage
d	Diameter (m)	KAP	Knitting aryl network polymer
		SIMP	Solid Isotropic Material with Penalization
Greek letters		FA	Fatty amines
α	Thermal diffusivity (m^2/s)	ODA	Octadecylamine
ρ	Density (kg/m^3)	BD/BM-CPCM	Bio-derived/bio-mimetic Composite PCM
θ	Dimensionless temperature	PW	Paraffin Wax
β	Coefficient of volumetric expansion (/K)	PPF	Pomelo Peel Foam
μ	Dynamic viscosity (kg/m.s)	SCG	Spent Coffee Grounds
ε	Emissivity	JPB	Jujube Pit Biochar
λ	Latent heat of fusion (kJ/kg)	FA	Fatty Acid
		DPMS	Dopamine-functionalized mesoporous silica
Abbreviation		AWSC	Activated Walnut Shell Carbon
NePCM	Nano enhanced PCM	WSC	Walnut Shell Carbon
TC	Thermal Conductivity	GS	Graphene Skeleton
MA	Myristic Acid	PCM	Phase Change Material
CTW	Chemically Treated Wood	CF	Copper foam
CLP	Carbonized Lemon Peel	TDA	Tetradecylamine
MP	Methyl Palmitate	CMSs	Copper Microspheres
BN	Boron Nitride	CA-LA	Capric-Lauric acid
CNCC	Carbonization Corn Cob	CDF	Calcined diatom frustules
SIMP	Solid isotropic material with penalization	TCES	Thermo-chemical energy storage systems
MWh	Mega Watt hour	LHES	Latent heat energy storage systems
HTF	Heat transfer fluid	SHES	Sensible heat energy storage systems
ROI	Return of Investment	WF	Wood-Flour
		CARM	Carbon microsphere

SHES materials are brick, rock, ceramic, cast steel, cast iron, concrete, water, synthetic oil, molten salt, mineral oil, and silicon oil. Despite its benefits, it is limited by a lower energy storage density, which necessitates a larger storage device to store large amounts of energy [17,18].

In the LHES, eutectic, inorganic, and organic mixes are all present, undergo cyclical phase changes when charging and discharging (Fig. 3 (a) and (b)). The advantages of the LHES system are its small size, isothermal characteristics when discharging, and increased energy storage capacity [19]. Knowing that LHES systems utilize the benefits of the alteration of chemical bonds in the material's mass structure, their energy storage density is far greater than that of SHES systems [18]. The proportion of renewable energy integration into the nation's energy system is steadily increasing in tandem with the gradual rise in worldwide energy usage [20,21], which also adds to the challenge of maintaining the stability of the energy network given its volatility and intermittent nature. Solid-liquid phase change energy storage has drawn considerable attention from researchers both domestically and internationally due to its many benefits, which include a high density of energy storage, minimal thermal shift during the energy storage process, and an easy-to-manage process (Fig. 4) [22–24]. As energy storage carriers, PCMs offer a wide range of application possibilities in electronics, building, solar thermal usage, and waste heat recovery system [25–32]. They may store or release enormous amounts of heat through melting or solidification.

PCMs can be classified as solid-solid, solid-liquid, solid-gas, and liquid-gas PCMs based on the phase shift states. They can be categorized as organic, inorganic, or eutectic based on their chemical makeups. Inorganic PCMs have a wide range of materials and phase transition temperatures, primarily including molten salt, metal, and alloy [33,34]. Inorganic PCMs have a lesser amount of volume change, exhibit greater latent heat of fusion per unit volume, are more readily available, and are less expensive. However, they come with the following drawbacks: poisoning, phase segregation, supercooling, inadequate thermal stability, and corrosion on metallic containers. The family of organic PCMs comprises alcohols, paraffin, fatty acids, aliphatic hydrocarbons, and polymers among others. The chain length as well as the functional groups affect the phase transition temperature, with a longer chain length indicating a greater phase transition temperature. Compared to inorganic PCMs, organic PCMs are non-corrosive, safe, and chemically stable. Furthermore, they exhibit no propensity to segregate or supercool, have a good latent heat of fusion, and are compatible with all metal vessels. However, because of their reduced phase change enthalpy and weaker thermal conductivity, they endure significantly [35]. For example, the low thermal conductivity of some salt hydrates (0.4 W/m.K to 0.7 W/m.K) [36] or, organic PCMs (0.15 W/m.K to 0.3 W/m.K) [37] limits their thermal response and performance effectiveness due to higher thermal resistance values.

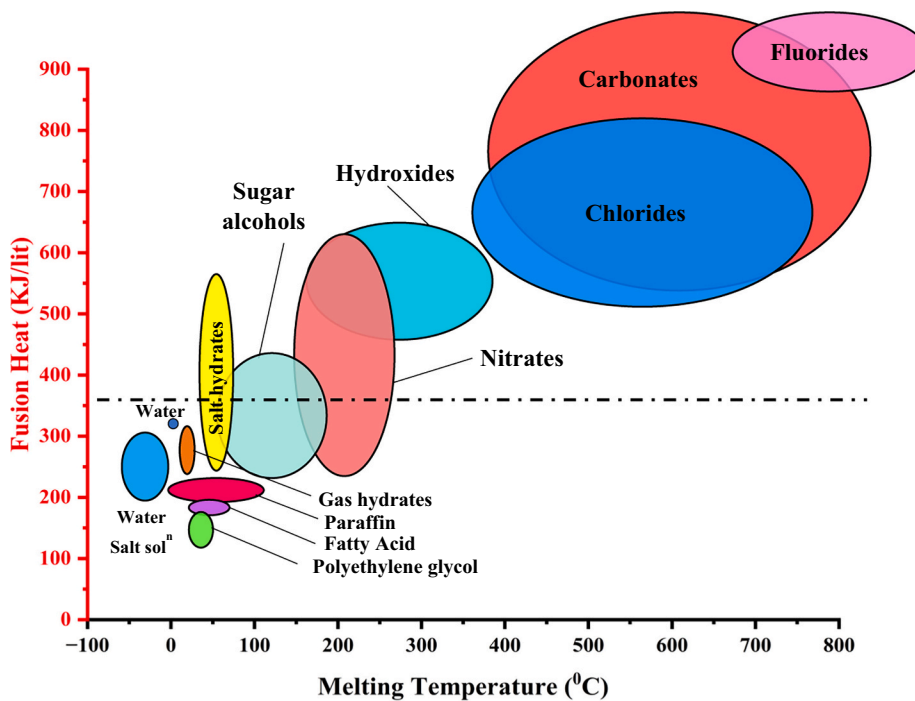A few investigators have, however, undertaken truly intriguing

Fig. 1. Classification of PCMs according to melting temperatures and fusion heat [6].
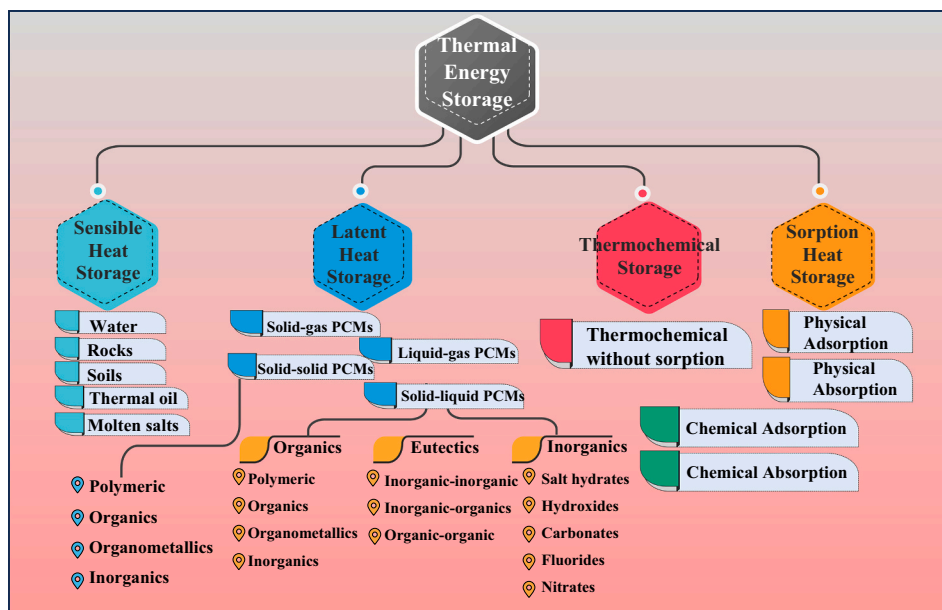

Fig. 2. Classification of Thermal Energy Storage materials.

efforts to enhance PCM properties with the incorporation of matrix materials which are inspired from nature or derived from it. Bio-derived and Biomimetic Composite Phase Change Materials (BD/BM-CPCMs) is able to regulate the temperature in a wide range of temperature differences. Moreover, they are of great indication to utilize green technology that is considered more sustainable than the other types of PCM composites. As the matrix materials of BD/BM-CPCMs are mimicked from nature this leads to high energy density and conversion efficiency, long life and operating cycles and versatility of the composite PCM. Therefore, in light of the foregoing talks, this article capitalizes on the chance to close the aforementioned gaps by providing an overview and assessment of the research on BD/BM-CPCMs for thermal energy storage

applications over the past few decades, as well as to suggest future directions. Besides, underlying scopes of BD/BM-CPCM in TES application based on enviro-economic aspects are depicted. Moreover, several heat transfer models are proposed to analyze phase transitions along with critical discussions on machine learning approach on multivariate and multi-objective optimizations from a technical, financial and environmental standpoint.

The precise organizational structure of this review can be summarized as follows: The originality of the work-study program has covered along with the main issues with PCM-based TES systems in Section 1. In Section 2, discussions are held regarding the latest property enhancement initiatives of various PCMs. In Section 3, different studies that are
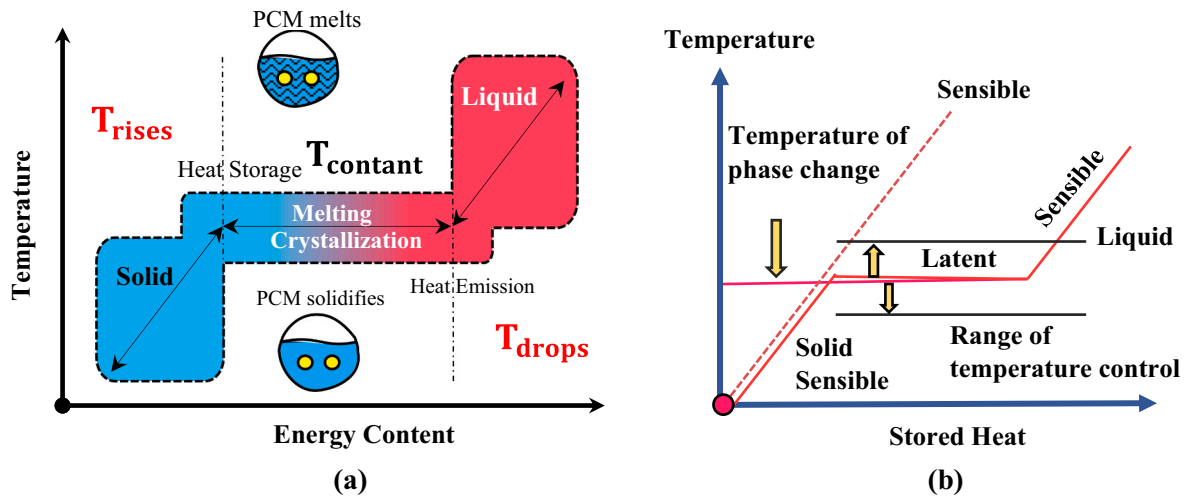
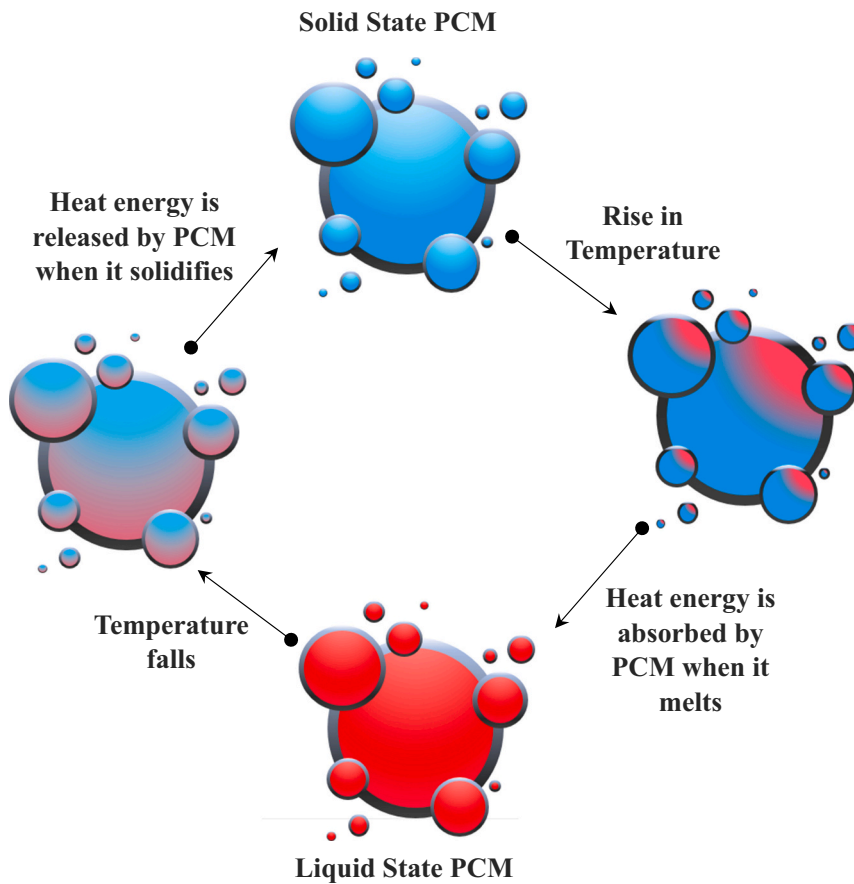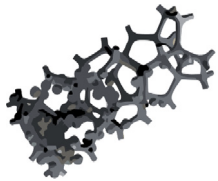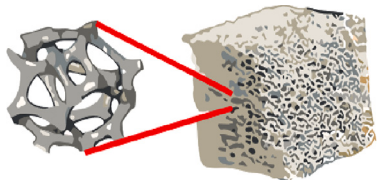**Fig. 3.** (a) Principles of phase change behavior of PCM, (b) graphical representation of phase change for PCM.
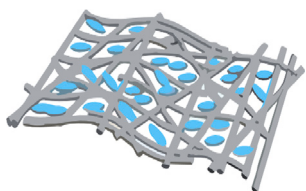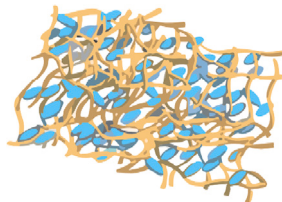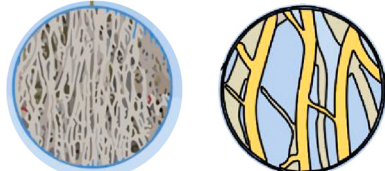

Fig. 4. Physical phase change mechanism upon cyclic heat absorption and release.

very much relevant to BD/BM-CPCM mentioning their preparation techniques, characterizations, and key findings are depicted and tabulated. Sections 4 and 5 discuss the enviro-economic aspects of TES with underlying scopes of BD/BM-CPCM in great extinct and numerical approaches to heat transfer during phase change along with multivariate and multi-objective optimizations from a technical, financial and environmental standpoint using machine learning techniques. Additionally, Section 6 expatiates the concluding observations and suggested future research directions.

2. Property improvement strategies

Incorporating nanoparticles to PCMs to increase their thermal conductivity is becoming more prevalent due to the rapid advancement of nanotechnology. The TES performance is greatly improved by the addition of a tiny quantity of the right conductive nanoparticles [38]. One of the most extensively utilized methods to improve the heat transfer rate in PCMs is the use of expanded surfaces. An expanded surface promotes natural convection within the system, enhances the

Table 1
Advantages and disadvantages of five matrices.

Matrix	Structure	Advantages	Disadvantages
Ceramic [58]		High sensible heat storage capacity. Wettable with PCM. Good dimensional stability. Excellent chemical and thermal stability. Good corrosion resistance. Low cost.	Frangibility.
Metallic [58]		Excellent thermal conductivity. Good mechanical strength. High porosity. Excellent thermal stability.	High cost. Corrosion issue. Insufficient wetting to PCMs.
Carbon [58]		Excellent thermal conductivity.	High cost. Less high temperature stability. Complex preparation process.
Polymeric [58]		Low packing rate of PCMs. Flexible. Low cost. High reproducibility and large-scale preparation.	Low thermal conductivity. Less thermal stability. Low applicable temperature, (<400 °C).
Bio-based matrix [59]		High temperature regulating capability. High energy conversion efficiency with the implementation with PCMs. Utilize green technology and more sustainable. Excellent thermal conductivity. Good corrosion resistance.	Complexity in analyzing of heat transfer mechanism.

rate of heat transmission, and strengthens thermal energy storing ability of PCM. The capability of PCM's heat transfer is dependent on the number, size, and configuration of fins in the TES, which is primarily a conduction and convection process. Numerous researchers have documented numerous techniques for improving thermal performance of PCM [39–42].

Due to high propensity for shape-stabilization issues over actual charging and discharging procedures of PCM, ineffective TES and the ensuing losses in material arise [43,44]. PCM encapsulation is recognized as one of the frequently employed techniques to ensure that the material has chemical and mechanical stability since it compensates for the change in volume throughout the phase transition process and prevents the corresponding phase separations concurrently [45]. It also makes it possible to produce appropriate PCM composites [46]. A metal foam with superior thermal conductivity, greater surface area, strength,

and stiffness is the absolute ideal metallic composite additive. With the solid skeleton's high intrinsic thermal conductivity and the curved channel's excellent mixed disturbance properties for heat transmission [47,48]. Numerous unique strategies, such as hybridizing and system cascading, have been put forth in studies to guarantee optimal TES operations. In TES applications, the cascaded PCM system is crucial. According to the need for abundant economics and a restriction on the amount of improvement, it is important to evaluate how different thermo-physical characteristics of PCMs affect the efficiency of heat transport.

3. Biomimetic composite PCMS

Typically, composite PCMs mix a PCM with porous fibers, particles, or skeletons that have a high thermal conductivity. Table 1 depicts the
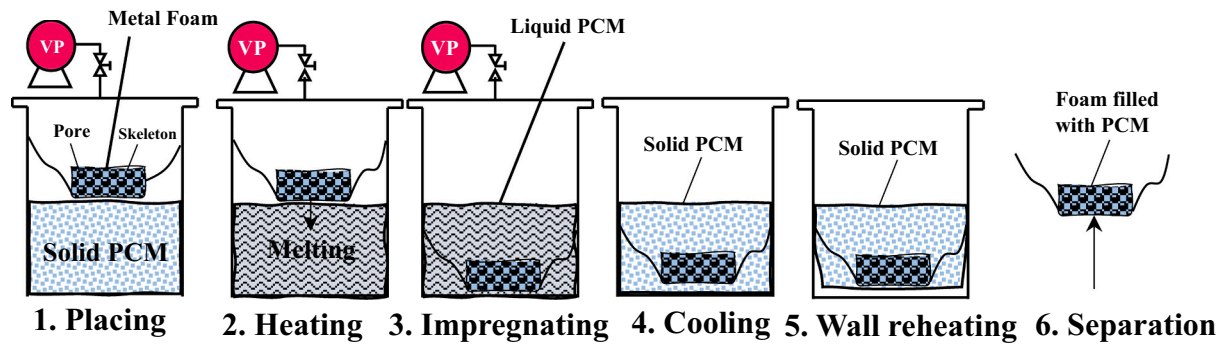
Fig. 5. Vacuum impregnation method for making PCM composite.

merits and limitations of five matrices. As a result, currently available biomimetic composite PCMs concentrate on creating porosity skeletons, fiber arrangements, or particle morphologies that are inspired by biological systems. Several unusual natural morphologies and structures, such as honeycomb structures, structure inspired from spider web, heterogeneous structures (such as animal tibiae and plant stems), and hierarchical structures (such as diatom frustules and loofah sponges) have drawn a great deal of attention since their stunning configurations. The research shows that tiny adjustments in latent heat of fusion can dramatically improve LHES performance by increasing the thermal conductivity of biomimetic composite PCMs several-fold (often surpassing 2 times). Additionally, biomimetic composite PCMs have generally strong thermal stability. Existing research suggests that even after several hundred cycles, the heat-storage capacity of these biomimetic composite PCMs may be sustained without appreciably declining.

3.1. Preparation methods: vacuum and melt impregnation method

Zhang et al. [49] prepared stearic acid (SA) and modified expanded vermiculite composite using direct vacuum impregnation method. In a glass beaker, a support matrix and solid SA were combined at a mass ratio of 10:1. The vacuum oven was heated at 80 °C under vacuum and linked to a vacuum pump to remove air, which melted the solid SA. Das et al. [50] attempted to prepare a total of four distinct PCM to biochar (water hyacinth biochar, WH 550) with several mass ratios. The PCM and biochar were placed in a glass beaker with an aluminum foil-covered mouth and heated in a hot air oven for 16 h at a predetermined temperature of 80 °C. The samples were removed from the oven after 16 h and allowed to cool naturally in the air until they reached room temperature. The carbonized lemon peel/n-Heptadecane (CLP/HD) composites were developed using a vacuum process by Hekimoğlu et al. [51] at various weight combinations. The HD was first melted at 40 °C and then mixed into a beaker with a specific quantity of CLP powder. Using a vacuum pump integrated-oven, this sol-gel was combined for 30 min with a mechanical stirrer before being vacuum processed to improve the impregnation ratio of PCM.

The graphene skeleton was fully submerged in the molten paraffin wax (PW) after placing a container containing the appropriate quantity of PW in an oven set at 65 °C for 0.5 h according to the study of Lin et al. [52]. After that the aerogel was completely impregnated with the melt using the process of vacuum impregnation, as shown in Fig. 6(a). The packed skeletons were able to be gradually cooled to room temperature to extract the PCCs. For instance, sw-GS/PW-1.0 has a loading of 1.0 vol % for sw-GS. Fig. 6(b) shows the SEM pictures of rGO aerogels made at several magnifications, unidirectional freeze–casting, radial freeze–casting techniques. According to the study of Chen et al. [53], melt impregnation was used to create the FAs/GS composites, with TDA and ODA being chosen as FA representatives as shown in Fig. 7(a) and (c). A certain grade of TDA (or ODA) powder is added to a 5 mL glass vial,

which is then baked at 80 °C to melt it entirely. The TDA (or ODA) was then allowed to permeate into the GS by adding a certain quantity of GS into the glass bottle above. Fig. 7(b) shows the SEM pictures of GS, TDA/GS, and ODA/GS.

The GO-BN mixes were transferred to a structured copper mold that could create multi-directionally aligned temperature gradients by Liu et al. [54] in order to change the orientation of the ice crystals when submerged in liquid nitrogen. As a result, after vacuum-assisted freeze-drying, the rationally created filler scaffold would be successfully produced (Fig. 8(a)–(e)). The GO sheets in the GO aerogel are arranged and precisely aligned in a centrosymmetric pattern along the radial direction, illustrated in Fig. 8(g), (h) and (i). The GO-BN sheets remain precisely aligned in a centrosymmetric arrangement even after being combined with plentiful BN. This can be attributed to the GO auxiliary-dispersion effect, which shows that the radial structure was successfully formed. Capric acid (CA), methyl palmitate (MP), lauryl alcohol (LA), and a combination of fatty acids from coconut oil and linoleic acid (CoFA-LA) were used in the study of Palanti et al. [55] to saturate the sapwood specimens. In an enclosed oven, CA, MP, and LA were impregnated for 3 h at 45 °C and 0.85 bar of pressure. In a sterilized vessel set at 60 °C, the wood samples were impregnated with CoFA-LA to guarantee the melting and vacuum pressure processes of the bio-based phase change material (BPCM) in building application.

By using the melt impregnation process, melted PCMs can be substantially assimilated by a porous matrix; nevertheless, the PCM does not completely fill the pores of the matrix, limiting the energy storage density. A method of vacuum impregnation was suggested to address this issue by most of the literatures stated above as shown in, Fig. 5. The supporting matrix is first subjected to vacuum using a vacuum pump integrated-oven for the process in order to eliminate air from the pores and filler from the fissures. The melted PCM at around 65 °C to 80 °C is fed into the vacuum system to permeate the supporting matrix for 30 to 60 min once adequate degassing has been accomplished [56,57]. Table 2 summarizes of the previously conducted studies to improve the thermosphysical properties of PCM utilizing bio materials.

3.2. Characterization and property variations

3.2.1. Thermal conductivity

From the study of Lin et al. [52], pure PW had a thermal conductivity of 0.19 W/m.K. Due to the PCM's low intrinsic thermal conductivity, heat conduction is limited, which results in inefficient energy storage and release. In contrast, when filler loading increased, the PCCs displayed larger cross-plane thermal conductivities. In particular, the cross-plane thermal conductivities of RD/PW, GS/PW, and sw-GS/PW demonstrated 1.21 W/m.K, 2.01 W/m.K, and 2.58 W/m.K, respectively, with 2.25 vol% filler, resulting in roughly 537 %, 958 %, and 1258 % enhancement in comparison to PW (Fig. 6(c) and (d)). The PW composites' in-plane thermal conductivity and augmentation with filler loading are shown in Fig. 6(e) and (f). Because the fillers were

Table 2

Summary of the previously conducted studies to improve the thermos-physical properties of PCM utilizing bio materials.

PCM/matrix	Method	Thermal conductivity improvement (W/m. K)	Change of Latent Heat from (J/kg)	Melting temperature from (°C)	Important findings	Reference
Stearic Acid/Modified expanded vermiculite	Vacuum impregnation method	0.21 to 0.52	219.53 to 134.31	68.77 to 67.12	Solid PCM to supporting matrix ratio is 10:1	[49]
Lauric–Stearic Acid/ Carbonized Corn cob	Vacuum impregnation method	0.228 to 0.441	199.6 to 148.3	37.5 to 35.1	Carbonized Corn cob PCM can reach a maximum of 77.9 wt% without leaking.	[60]
BSiC/paraffin	Genetic assisting method	Up to 35	Up to 309	Narrow changes of 3 °C	At a porosity of 66 %, BSiC/paraffin exhibits a high thermal conductivity of 40 W/m.K.	[61]
PEG/Jujube pit biochar	Vacuum impregnation method	0.280 to 0.630	194.77 to 108.2	51.4 to 52.0	Using an in-situ reduction technique, copper microspheres were introduced to a carbon-based adsorbent	[62]
PCM-water hyacinth biochar and aluminum powder	Direct impregnation method	(0.0191 ± 0.0109) to (0.349 ± 0.0053)	Up to 179.4	Up to 57.67	The ratio of PCM to biochar (wt/wt%) is determined to be 6:4, exhibiting the least amount of PCM leaking through the composite	[50]
PEG/ZSM-5	Vacuum impregnation method	0.22 to 0.54	192.6 to 76.4	59.5 to 56.3	The findings of exudation stability tests demonstrated that PEG doping may reach up to 50 % weight percentage without leaking and with adequate thermal stability.	[63]
Capric–Lauric acid/ Diatomite	Vacuum impregnation	Up to 0.467	141.5 to 87.33	19.09 to 23.61	After 200 thermal cycles of thermal cycling tests, the composite demonstrates good thermal reliability.	[64]
Fatty acid/Wood–flour	Direct impregnation method	–	Up to 102.6	–	Latent heat indicating as a potential TES material for applications in energy-efficient buildings with PCM.	[65]
Loofah-derived SiC ceramics	Vacuum impregnation method	Up to 20.7	Up to 424	–	When compared to pure PCMs, the solar absorptance (95.25 %) is greatly increased.	[59]
Starch-derived porous SiC ceramics	Freeze-drying method	Up to 30	Up to 331.56	–	Thermal conductivity and thermal energy retention density of SiC/paraffin CPCMs only marginally declined by 2.80 % and 2.75 %, respectively, throughout 500 more heating-cooling cycles.	[66]
Palmitic acid/Pinecone char	Vacuum impregnation method	0.2731 to 0.3926	84.74 to 219.63	62.07 to 59.25	Leakage testing reveals that PCM: Biochar (6:4) shows optimum performance	[67]
Nacre-like ceramics embedded (TiN) nanoparticles	–	25.63	Up to 157.93	–	TiN NPs should be concentrated to 0.01 wt% concentrations below and above this results in poor optical absorption and sluggish heat dissipation rates.	[68]
PEG/Almond shell biochar	Vacuum impregnation	0.427 to 4.5	205.7 to 158.8	58.8 to 56.5	Highest thermal conductivity is 10 times higher than the pristine PEG	[69]
PEG/EG-CNF-BN	Solution blending method	Up to 10.83	Up to 79.46	–	The film's phase transition enthalpy can continue to be 79.46 J/g and nearly remain unchanged even after 40 heating-cooling cycles, according to DSC data.	[70]
PW/lotus stem bio-composite	Impregnation process	–	–		With no weight loss, composite materials can sustain temperatures of up to 320 °C.	[71]
PEG/Bio- based PPF @ MXene nanosheets	Simple impregnation process	0.25 to 0.42	165.6 to 157.9	Up to 62	PEG loading in form-stable composite phase change materials rose from 86.9 % to 96.2 % (wt/wt)	[72]
PEG/SCGs@RGO	AA reduction and vacuum-assisted impregnation	0.300 to 0.336	176.1 to 104.7	63.7 to 63	The thermal parameters, chemical properties, and crystallinity of PEG/SCGs@RGO have not shifted despite 100 cycles of both heating and cooling.	[73]
MP/AWSC	Vacuum impregnation method	0.38 to 0.93	Up to 26.65	Up to 138.82	The increase in the thermal conductivity of MP with AWSC was 57.89 %.	[74]
MA/CTW-2	Vacuum impregnation method	–	Up to 179.1	56.1 to 55.7	When it comes to managing temperature and TES during the light-to-thermal conversion procedures, MA/CTW-2 is superior.	[75]
MP/WSC	Vacuum impregnation method	0.38 to 0.97	Up to 26.27	Up to 108.32	The increase in the thermal conductivity of MP with WSC was 89.47 %.	[74]
PW/CTW-2	Vacuum impregnation method	–	Up to 181.9	No change	–	[75]
n-Heptadecane/CLP	Vacuum technique	0.26 to 0.46	Up to 141.8	Up to 19.79	CLP/HD composite PCM can be used to create new, environmentally friendly, energy-saving construction materials at a reasonable price.	[51]
PEG/CTW-2	Vacuum impregnation method	–	Up to 132.6	56.3 to 55.8	–	[75]
PU/WP PCM	Vacuum impregnation	–	Up to 134.2	Up to 63.5	Relative enthalpy efficiency reaches to 98.7 %	[76]
Biomimetic Leaf Hierarchical Porous Structure	Numerical	–	–	–	The largest increases in liquid percentage and completion rate are seen at 25 Pa pressure drop decrease (20.3 % and 36.6 %, respectively). The greatest lowering of the above-melting-point (MP) thermocline is likewise 51.7 %.	[77]

Table 2 (*continued*)

PCM/matrix	Method	Thermal conductivity improvement (W/m.K)	Change of Latent Heat from (J/kg)	Melting temperature from (°C)	Important findings	Reference
PEG/DPMS	Hydrothermal approach	Up to 0.491, which is 1.89 times larger than PEG	Up to 69.77	Up to 56	The fusion and solidification enthalpies of 70 wt% PEG/DPMS increased from 47.25 J/g and 34.96 J/g to 69.77 J/g and 67.54 J/g, respectively, after dopamine modification.	[78]
PW/sw-GS	Vacuum impregnation	Up to 2.58, with the improvement 1260 %	172.5	53.5	sw-GS/PW demonstrates significant gains in both in-plane and cross-plane thermal conductivity of around 1260 % at an ultra-low filler loading of 2.25 vol%.	[52]
PCM (PW)/KAPs-CF	Vacuum impregnation	Up to 55.37	105.60	58.16	The inclusion of paraffin wax in the combination of reactions facilitates the development of the straight KAPs unit, hence enabling the pseudo-one-dimensional polymeric unit to exhibit favorable swelling and good encapsulation properties.	[79]
FAs (TDA & ODA)/GS	Vacuum impregnation	0.2381 to 0.3551 and 0.4956	293 to 303	36.3 to 51.9	The thermal conductivities of the FAs/GS composites are improved; that is, they are approximately 164.4 % to 176.7 % greater than those of pure FAs.	[53]
PEG/BN	Vacuum impregnation	Up to 2.94	Up to 147.5	–	The composite material may achieve an impressive 85.1 % photothermal energy conversion efficiency when exposed to a localized light source.	[54]
PEG/CARM-Cu	Vacuum impregnation method	Up to 0.497, which is 1.89 times larger than PEG	Up to 101.50	60.20	The results of the thermal cycling test showed that PEG/CARM-Cu-2 exhibited outstanding thermal reliability.	[80]
PEG2000/Bionic bone hierarchical porous AlN ceramics	Gel foaming method	0.42 to 17.16	Up to 88.73	Up to 54.75	$1.5 \times 10^4 \, m^2.K/W$ is the impedance to heat transfer between the PEG2000-filled interior and the AlN skeleton.	[81]

distributed randomly, RD/PW showed isotropic thermal conductivity. As shown in Fig. 7(d) and (e), the thermal conductivity of the synthesized PCM composites and pure FAs may be visually compared at three different temperature points based on the study of Chen et al. [53]. The thermal conductivity values of pure TDA at 25 °C, 35 °C, and 45 °C is 0.2381 W/m.K, 0.2132 W/m.K, and 0.2467 W/m.K, respectively. On the other hand, the thermal conductivity of TDA/GS is quite high, reaching up to 0.3443 W/m.K, 0.3241 W/m.K, and 0.3551 W/m.K, respectively. It is higher than the control by about 144.6 %, 152.0 %, and 143.9 %, respectively. Comparable to this, the maximum thermal conductivity values for ODA/GS are 0.4944 W/m.K, 0.4189 W/m.K, and 0.4956 W/m.K, whereas those for pure ODA are 0.2899 W/m.K, 0.2371 W/m.K, and 0.3015 W/m.K at 25 °C, 40 °C, and 50 °C, respectively.

A flexible phase change film with stabilized shape is created by He et al. [70] using biodegradable and environmentally friendly cellulose nanofibers (CNF). Polyethylene glycol (PEG), which has been held in the porous expanded graphite (EG) by vacuum absorption, is used as a phase-change component in the film. The CNF serves as a supporting material and a substance that forms films. The cooperation of cellulose and EG results in the stability of form. Boron nitride (BN) improves the produced film's thermal conductivity. When compared to PEG/EG/CNF-1, the thermal conductivity of PEG/EG/CNF-4 is nearly two times higher at 5.18 W/m.K at a 7 % EG loading. Due to the highly aligned lamellar structure, the PEG/EG/CNF-based composite film demonstrates extremely anisotropic thermal conduction properties, which can reach 10.83 W/m.K. A new bio-based pomelo peel foam (PPF)/PEG composite PCM that is further modified with modest loadings of MXene nanosheets was conceived and created by Sheng et al. [72]. Fig. 9 shows the digital images of (a) fresh pomelo and (d) dried PPF, SEM images of (b) dried PPF and (c) PPF@MXene-4. Fig. 9(e) shows the diagrammatic representation of the conversion and storage of light to heat. The thermal conductivity of FCPCM-2, FCPCM-3, and FCPCM-4 are enhanced to 0.28 W/m.K, 0.35 W/m.K, and 0.42 W/m.K, respectively, with increasing MXene loading (Fig. 9(f)). Nevertheless, an optimal three-dimensional heat transmission network fails to appear within FCPCMs due to the comparatively low expansion values of the composite material itself, which are possibly connected to lower MXene loadings. The exceptionally high thermal conductivity of MXene nanosheets that have been

consistently disseminated throughout the PEG matrix and properly ingested on the PPF structure is responsible for an upsurge in thermal conductivity.

An innovative and inexpensive biochar-PCM based hybrid LHES was examined by Das et al. [50]. Aquatic invasive weed species were used to manufacture the biochar in batches (Fig. 10(a)). Thermal conductivity of the PCM was increased up to 13.82 times with the inclusion of biochar made by water hyacinth as a supporting matrix and even further increased by 17.27 times more than that of the PCM alone when aluminum metal powder was added (Fig. 10(b)). Shape-stabilized composite phase change materials (ss-CPCMs) with improved thermal conductivity were developed by Zhang et al. [49] using modified expanded vermiculite (MEV) and SA. The SA/EVC ss-CPCMs' thermal conductivity was 0.52 W/m.K, which represented a 52.9 % improvement over that of the SA/MEV ss-CPCMs. In order to achieve effective, quick, and portable solar TES, Liu et al. [61] improved phase change composites based on bamboo-derived silicon carbide (BSiC) eco-ceramics. Fig. 11 illustrates (a) the concept of solar thermal storage and the technique of fabricating BSiC ceramics using phase change composites; (b) a SEM picture; and (d) an infrared picture of paraffin and BSiC/TiN/paraffin placed under direct solar light. At a porosity of 66 % and a paraffin content of 96 %, BSiC/paraffin exhibits a high thermal conductivity of 40 W/m.K with no discernible deterioration after 2500 cycles. BSiC/LiOH-LiF composites are produced for high-temperature applications with a high thermal conductivity of 35 W/m.K (Fig. 11(e)).

Wen et al. [64] used the vacuum impregnation approach to create a novel form-stable composite PCM CA-LA/Diatomite by mixing a eutectic combination of capric-lauric acid (CA-LA) as the PCM and diatomite as the supporting material. Furthermore, EG was added to the hybrid to boost its efficacy of heat transmission. The findings indicated that the thermal conductivity of the composite increased as time passed by 39.7 %, 61.6 %, 77.6 %, and 114.2 %, respectively, for EG portions of 3 %, 5 %, 7 %, and 10 %. Incorporating nano-particles with PCM can uplift the thermal conductivity of the PCM. On the contrary, from Fig. 12, it is seen that the bio-mimetic and bio-derived materials pave the thermal conductivity of PCMs in a huge margin. According to the proposed study (Fig. 13(a)–(c)) of Xu et al. [59], adding loofah-derived SiC foam increases thermal conductivity of PCM from 0.2 W/m.K to 17 W/m.K
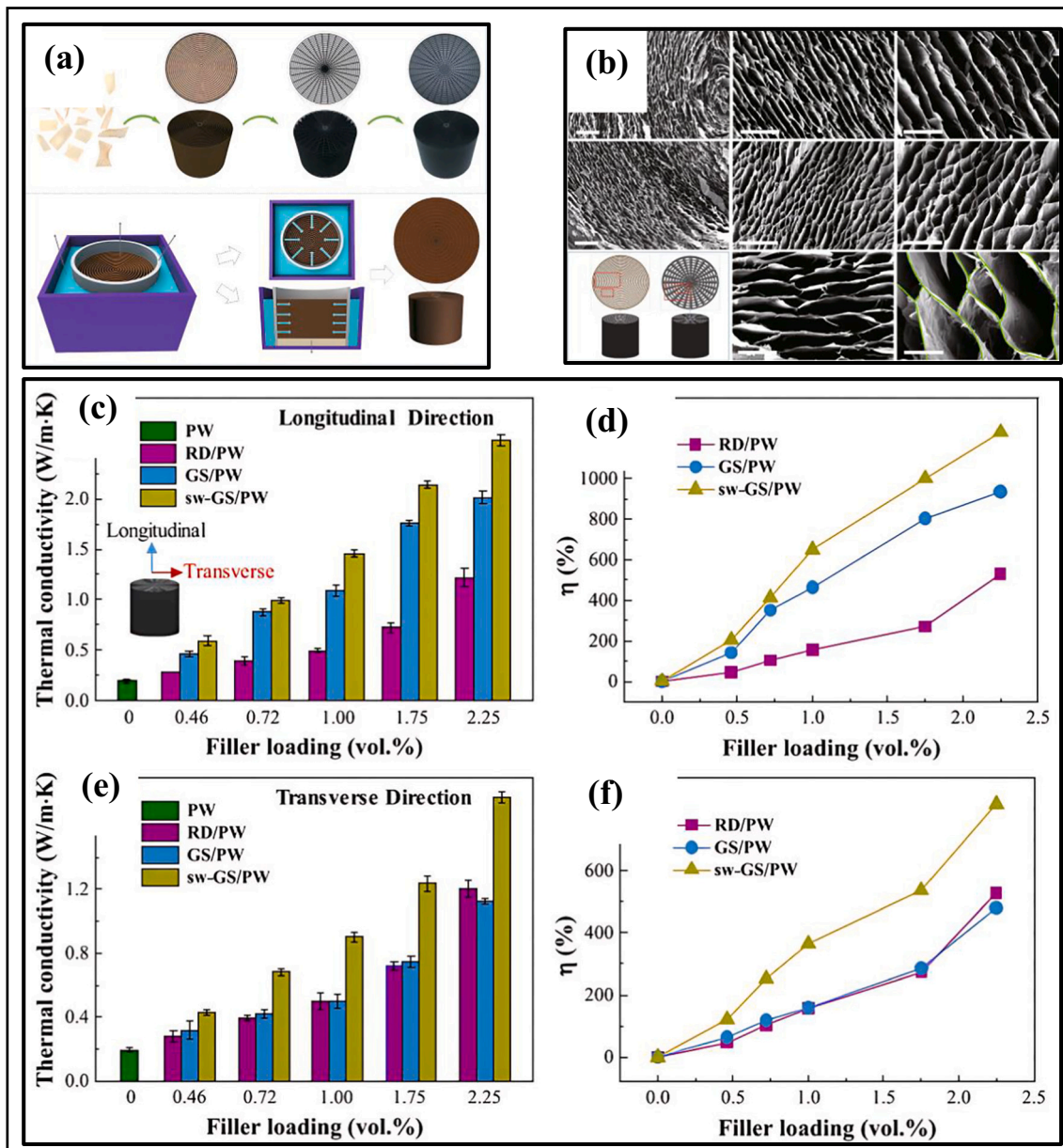
Fig. 6. (a) Diagram showing the steps involved in making a polymer composite, a spider web made of graphene skeleton and paraffin wax (sw-GS/PW), (b) SEM pictures of Reduced Graphene Oxide (RGO) aerogels made at several magnifications, unidirectional freeze–casting, radial freeze–casting techniques, (c) Thermal conductivity comparison and (d) enhancement in longitudinal (cross-plane) direction of PW composites; inset in (e) illustrates the thermal conductivity orientations for PW composites., (f) Thermal conductivity improvement in PW composites across the transverse (in-plane) orientation [52].
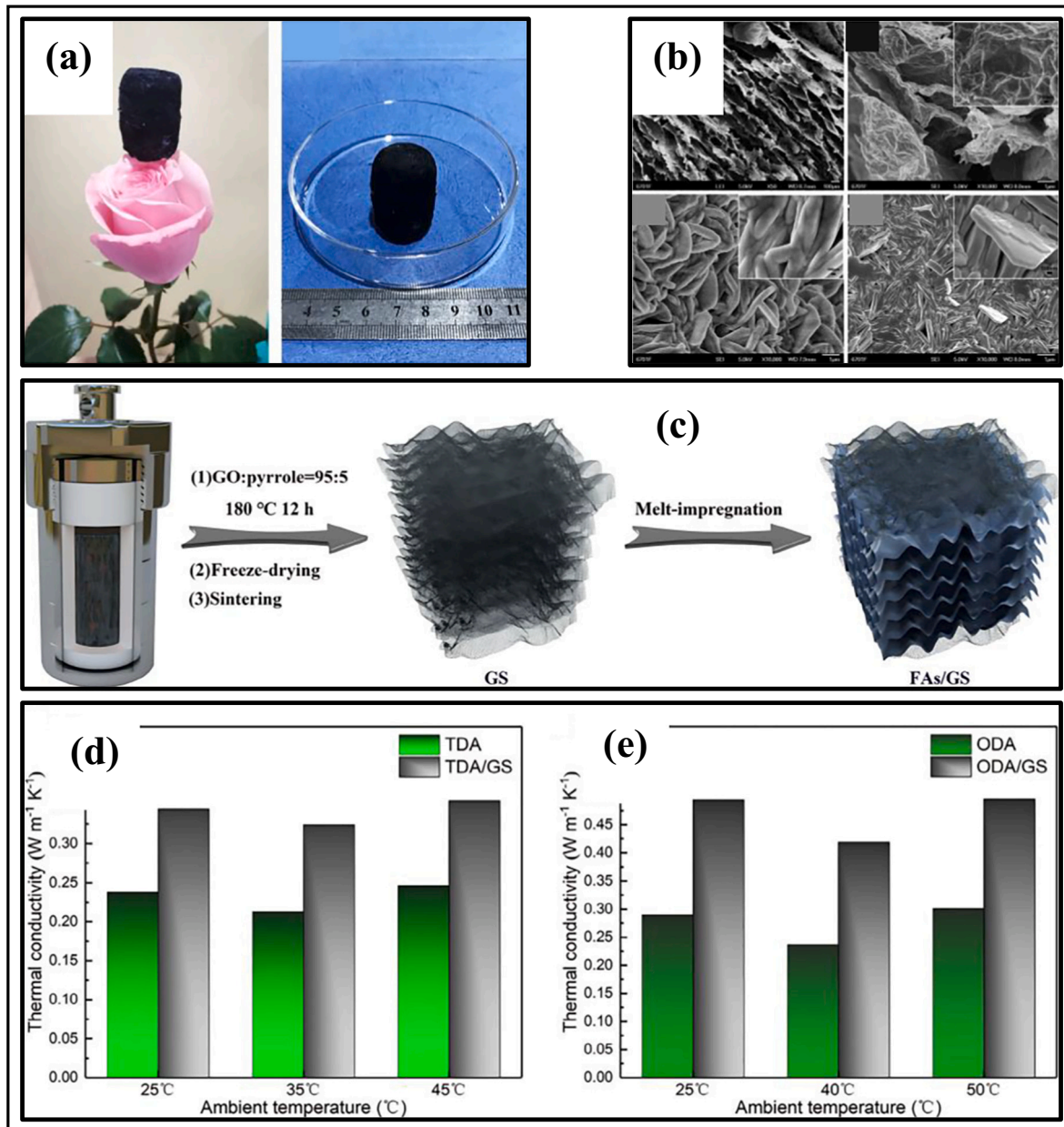
Fig. 7. (a) The digital photographs of Graphene Skeleton (GS), (b) SEM pictures of GS, Tetradecylamine/Graphene Skeleton (TDA/GS), and Octadecylamine/ Graphene Skeleton (ODA/GS), (c) pathway for Fatty Acid/Graphene Skeleton (FAs/GS) synthesis, the temperature-dependent thermal conductivity of (d) pure Tetradecylamine, Tetradecylamine/Graphene Skeleton and (e) pure Octadecylamine, Octadecylamine/Graphene Skeleton [53].

(CPCMs-80). The resulting system has a low operating temperature of 51 °C and an inadequate energy storage density of 70 kJ/kg.

The PCM-honeycomb composite structure's thermal conductivity was determined to be 2.08 W/m.K in a study by Xie et al. [82], and the numerical estimates' temporal temperature changes at the top and bottom sides aligned well. According to the set-up of Liu et al. [83], heat transport networks that resemble leaf veins improve the PCMs' capacity to absorb heat. As shown in Fig. 14(a) the structure and operation of natural and synthetic PCMs are compared, (b) physical model for heat dispersion, and (d) experimental platform. Given the need for reliable design criteria to create heat transmission networks, a novel optimization criterion that imitates the formation of leaf veins was proposed. The requirement was combined with an original flexibility-oriented optimization framework to create a generation conceptualization approach. The analogous conductivity of the yielding design was 298.31 % of the metal-foam-enhanced PCM's conductivity as well. In the meantime, the

generating design's conductivity was at least 17.32 % better than that of the solid isotropic material with penalization (SIMP) designs. Therefore, a design that adheres to the inherent branching law exhibits good heat absorption with increased thermal conductivity.

Song et al. [66] suggested starch-derived porous SiC ceramics to concurrently attain high heat conductivity and stop PCM leakage as shown in Fig. 15(a), (b) and (c). Gaining from directed pore architectures and thick grains made possible by simple directional freeze-drying of starch in conjunction with the liquid silicon infiltration technique, porous SiC ceramics with high thermal conductivity of 30 W/m.K at high porosity of 80 % are achieved (Fig. 15(d)). After 500 repeated heating-cooling cycles, the thermal conductivity and thermal energy storage density of SiC/paraffin composite PCMs (CPCMs) only marginally decreased by 2.75 % and 2.80 %, respectively.
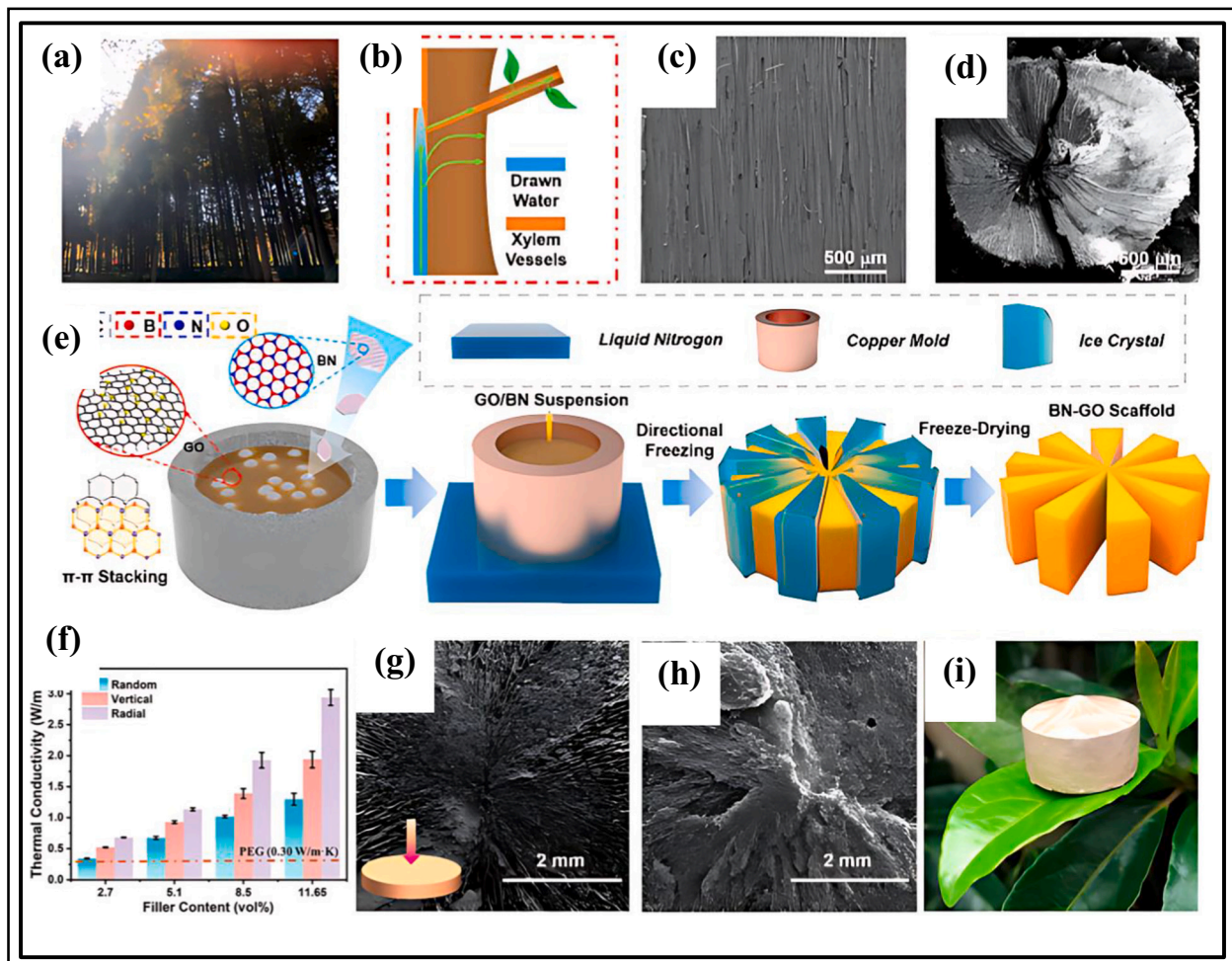
Fig. 8. (a) An optical image including tall conifer trees. (b) A diagram showing how water moves through fir trees. (c) Conifer plant longitudinal section and (d) cross-section having channels that are oriented radially and vertically, respectively. (e) Schematic diagram to generate a graphene oxide (GO)- Boron Nitride (BN) scaffold with bioinspiration. (f) Hot-disk analysis measurement of the PEG/BN composite's thermal conductivity. (g) A pure GO scaffold's cross-sectional morphology, and (h) a GO-BN scaffold made using the earlier described technique. (i) The optical image of the GO-BN scan [54].

3.2.2. Latent heat

As per the Li et al. experiment [63], the produced PCMs have a latent heat of 76.37 J/g. For the innovative composite PCM CA-LA/Diatomite proposed by Wen et al. [64], it was found that the material melted at 23.61 °C with a latent heat of 87.33 J/g and solidified at 22.50 °C with a latent heat of 86.93 J/g. In summary, it is found that the thermal enthalpies of melting CA-LA and CA-LA/D are, respectively, 141.50 J/g and 87.33 J/g. For CA-LA and CA-LA/D, the corresponding thermal enthalpy of freezing is 86.93 J/g and 140.30 J/g. Because of this, the CA-LA/D is suitable for thermal energy storage. Wood-flour (WF) was chosen by Liang et al. [65] as the supporting material in the direct impregnation approach used to create the composite fatty acid (FA)/WF form-stable PCMs. High latent heats and an appropriate range of phase transition temperatures were present in the created FA/WF CPCMs, especially the HW-FSPCM, whose maximal latent heats during the melting and freezing processes were 102.6 J/g and 103.5 J/g, respectively.

Balaji et al. [71] developed a bio-composite using epoxy resin and lotus stems as natural fiber reinforcement. To increase the lotus stem's potential for storing thermal energy, PCM was wax inserted into it. The epoxy resin composite was then reinforced with lotus fiber impregnated with wax. To create a cuboid block, a total of 6 numbers of bio-composite plates were created. In a thermal behavior test, it was shown that a single plate of bio-composite had a thermal energy storage capacity of 13.08 kJ and a bio-composite cuboid block had a thermal

energy storage capacity of 19.22 kJ. According to Sheng et al. [72], PEG inform-stable composites phase change materials (FCPCMs) were loaded at a rate of 96.2 wt% (FCPCM-2, FCPCM-3, and FCPCM-4) compared to 86.9 wt% (FCPCM-1). This substantially improved the light-to-thermal efficacy of conversion. The study by Hu et al. [73] states that the m values of PEG/SCGs@0RGO, PEG/SCGs@1RGO, PEG/SCGs@3RGO, and PEG/SCGs@5RGO are 93.95 %, 97.86 %, 98.47 %, and 98.60 %, respectively. Hekimoğlu et al. [74] in a distinct study show that WSC/MP and AWSC/MP composites display melting temperatures of 26.27 °C and 26.65 °C, respectively, and latent heats of 108.3 J/g and 138.1 J/g. Hekimoğlu et al. [51] produced a leak-proof CLP/HD composite PCM with a melting temperature of 19.79 °C and an LHS capacity of 141.8 J/g.

Wu et al. [84] used ship-shaped (SS) diatom (Pennales) frustules to create composite ss-PCMs with high phase change enthalpy and high polyethylene glycol (PEG) absorption capacity. The schematic diagram for the creation of ship-shaped diatom frustules ss-PCMs, the SEM pictures of the PEG/400CDF that were made, and the XRD pattern of the 400 CDF are all displayed in Fig. 16 (a–c). The resultant PEG/400CDF composites were loaded with 72.7 % PEG4000 and displayed a latent heat value of 128.9 J/g for melting and 136.7 J/g for freezing (Fig. 16 (d)). Up to 97.7 % of relative enthalpy efficiency is achieved for the ss-PCMs -based composite and display a better thermal and chemical stability even after 200 thermal cycles. For the phase transition material inspired by the sponge gourd and proposed by Liang et al. [85], the
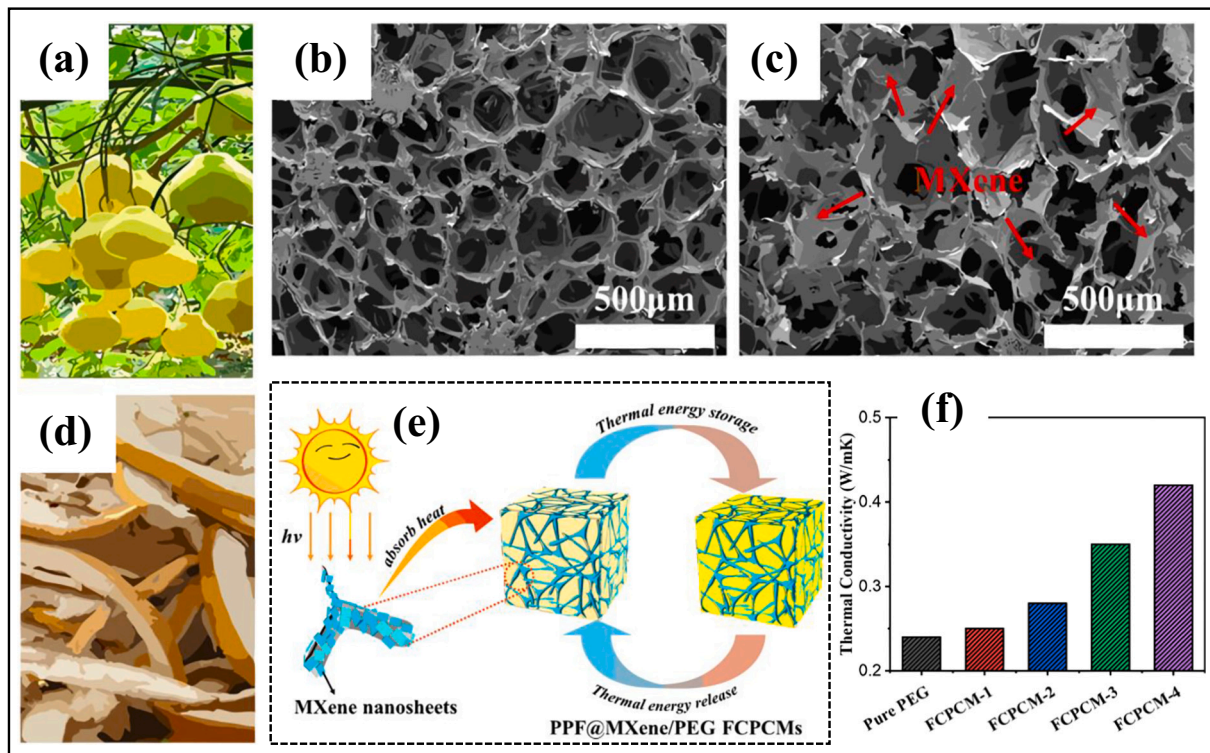
Fig. 9. Digital images of (a) fresh pomelo, SEM images of (b) dried Pomelo Peel Foam (PPF) and (c) PPF@MXene-4, (d) dried PPF (e) diagrammatic representation of the conversion and storage of light to heat, (f) The thermal conductivity of pure polyethylene glycol (PEG) and obtained form-stable composites phase change materials (FCPCMs) [72].

latent temperatures of melting (Hm) and crystallization (Hc) of PW/EG@GO are 158.5 J/g and 156.1 J/g, respectively. The figures are incredibly high—the final three are about 100 %—and are attainable through the use of phase change energy storage materials compliant with passive heat absorption criteria in practical applications. The relative enthalpy efficiency of diatom-based biomass/polyethylene glycol composites can reach 98.1 % [86].

3.2.3. Melting temperature

In order to develop a unique leak-proof composite PCM, Hekimoğlu et al. [51] proposed a framework that included CLP and HD as a solid-liquid PCM. The thermograms clearly show that the leak-proof CLP/HD composite PCM's heating and cooling thermal performance is remarkably close to that of pure HD based on the testing results for both of these materials. Pure HD's solid-solid phase transition and melting point were determined to be 9.36 °C and 19.86 °C, respectively. From the study by Hekimoğlu et al. [74] showed that the WSC/MP and AWSC/MP's melting and freezing temperatures reduced to 25.98 °C/24.37 °C and 25.98 °C/25.23 °C, respectively. These drops in WSC/MP and AWSC/MP's melting and freezing points are 0.29 °C/0.58 °C and 0.67 °C/0.27 °C, respectively. These alterations can be attributed to potential variations in the physicochemical interactions between the supporting material and PCM across the heat cycles. The melting temperature of the PCM-biochar composite, which is somewhat lower than that of pure PCM, is found to be 57.67 °C according to the DSC test results from Das et al. [50]. This is because adding biochar causes the crystal nucleus to shrink. Zhang et al. [60] reported that the melting temperatures of LA-SA and LA-SA/CNCC FS-CPCMs were 37.5 °C and 35.1 °C, respectively. Their respective freezing points were 29.9 °C and 29.7 °C. The little decrease in phase transition temperature is caused by the weak attraction between LA-SA molecules and the inner surface wall of the porous supporting matrix. Wen et al. [64] used a eutectic combination of CA-LA as the PCM and diatomite as the supporting material to generate a CPCM CA-LA/Diatomite using the vacuum impregnation

process. The findings showed that the melting point of the composite material was 23.61 °C. According to the study by Liang et al. [65], the decrease in crystal nucleus brought about by the incorporation of WF is a consequence of the LA/WF composite's decreased melting temperature compared to natural LA and the LA/WF composite form-stable PCM's larger supercooling degree of 3.5 °C compared to 1.4 °C for pure LA.

3.2.4. Energy storage efficiency

The solar thermal energy storage efficiency can be defined as follows:

$$\eta = m \frac{\Delta H}{P.S.\Delta T}$$

where m refers to the mass of paraffin, H is the sample's latent heat, P is the sun irradiation flux, S denotes the sample's bottom area, and t is the duration between phases. According to the study of Liu et al. [61], as solar irradiation varies between 1.32 W/cm^2 and 1.62 W/cm^2, the solar TES efficiency of BSiC/TiN/paraffin increases from 78.8 % to 91.1 %. Phase change takes place over a period of time that decreases with increasing solar radiation, from 23.6 s at 1.32 W/cm^2 to 16.6 s at 1.62 W/cm^2. That instance, more solar radiation can minimize heat losses and shorten the time it takes for phase transitions, increasing efficiency. Additionally, the use of TiN nanoparticles increases solar absorptance, which lowers light reflection losses and optimizes solar-thermal energy utilization. The rapid heat transfer from the bottom irradiation surface to the top surface, made possible by high thermal conductivity, may guarantee a high energy storage efficiency.

According to Xu et al.'s study [59], when solar radiation increased from 8 to 18 kW/m^2, the solar TES efficiency increased considerably from 22.9 % to 76.62 %, but only marginally from there to 79.80 % when solar radiation increased from 18 to 27 kW/m^2 (Fig. 11(c)). This is so that by reducing the phase-transition length, increasing solar irradiation can decrease the ratio of heat loss. When the solar radiation is 8 kW/m^2, 10 kW/m^2, 13 kW/m^2, 18 kW/m^2, and 27 kW/m^2, the
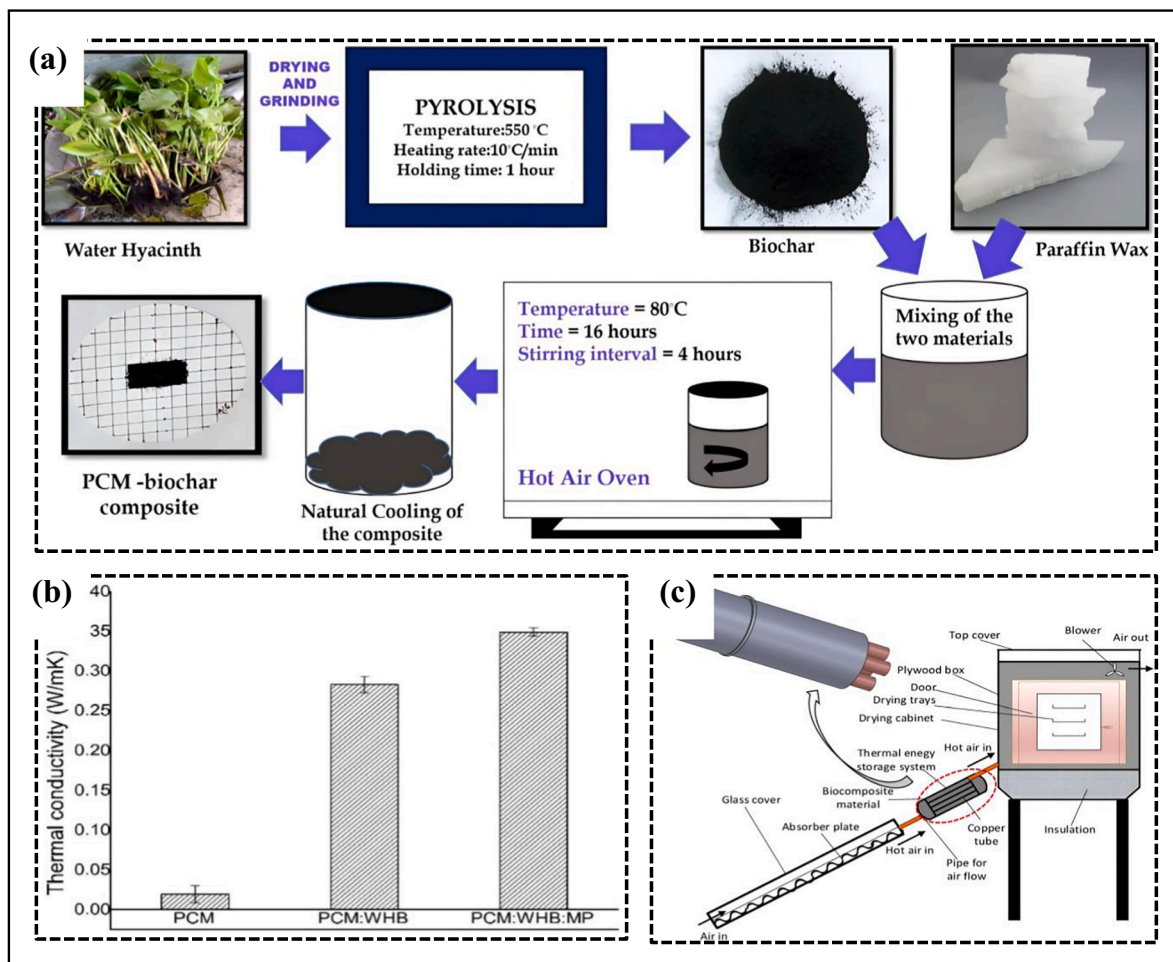
Fig. 10. (a) Procedures for preparing a composite, (b) thermal conductivity of the samples PCM with water hyacinth biochar (WHB), (c) diagram showing the thermal energy storage system with solar dryer [50].

corresponding charging times are 22 s, 24 s, 36 s, 70 s, and 143 s. Sheng et al. [56] discovered a unique non-freezing plant species, Lobelia telekii, may retain solar thermal energy through the day and discharge latent heat at night to prevent freezing in nature as shown in Fig. 17(a) and (b). It is found at high altitudes. In Lobelia telekii, there is a liquid that can be regarded as a natural PCM that both retains and releases thermal energy as shown in Fig. 17(c) and (d). In order to integrate solar-thermal transformation with thermal energy storage, they created round-the-clock SPCMs made of EG, paraffin, and polydimethylsiloxane (PDMS). Sheng et al. [56] determined that the storage efficiency was 81.04 % during the time when the composite was heated from 15 °C to 8 °C under simulated solar radiation, with a light intensity of 1000 W/m^2. This equates to an enthalpy change of 95.01 J/g. The temperature variation of the SPCM exterior under solar radiation (100 m.W/cm^2) at a surrounding temperature of −12 °C is shown in Fig. 17(e).

3.2.5. Thermal stability

The thermal stability of the sample was measured by TG by He et al. [70] and about 215 °C is the starting breakdown temperature (T5%), which is mostly due to the decomposition of cellulose, at which mass loss is 5 %. The high intrinsic heat capacity of the BN, which preferentially absorbs heat to delay the volatilization of the polymer chains, can be used to explain the improved thermal stability. Furthermore, 2D nanosheets BN may act as an isolator between the matrix and surface and a mass transmission obstacle whenever the temperature is elevated to the matrix's decomposition point, hence postponing its eventual degradation. Furthermore, his team discovers that even after prolonged heating

to the PEG melting point, the PCM films may retain their original shape and no PEG leaks from the matrix, showing that the created PCM films have exceptional phase change stability.

In order to create a unique leak-proof composite PCM, Hekimoğlu et al. [51] proposed a framework that included carbonized lemon peel (CLP) as well as n-Heptadecane (HD) as a solid-liquid PCM. After 1000 heating-cooling cycles, the composite PCM revealed remarkable thermal deterioration stability. According to the study of Das et al. [50], PCM degradation had taken place in a single step starting at about 135 °C and reaching its maximum level of degradation at 250 °C. Moreover, the thermal stability of the composite seems to be satisfactory. Furthermore, compared to the composite, PCM lost weight by around 99.1 %. Concerning surface tension, capillary forces, and other forces inherent in the substances utilized to produce the composite, the values achieved are smaller than those achieved in the past. It should be noted that the presence of these forces not only helps shape the composite but also improves the material's thermal stability. According to a study conducted by Li et al. [63], PCMs that had been made showed outstanding thermal stability below 155 °C, which is regarded as greater than its phase transition temperature. Meanwhile, the PEG is disintegrating, which is the cause of the sudden weight loss that occurred at a temperature of roughly 250 °C. The residual masses of each sample were calculated, and the results revealed that the PEG doping ratios of each sample as it was prepared were all in good accord with the default value.

3.2.6. Chemical stability and solubility

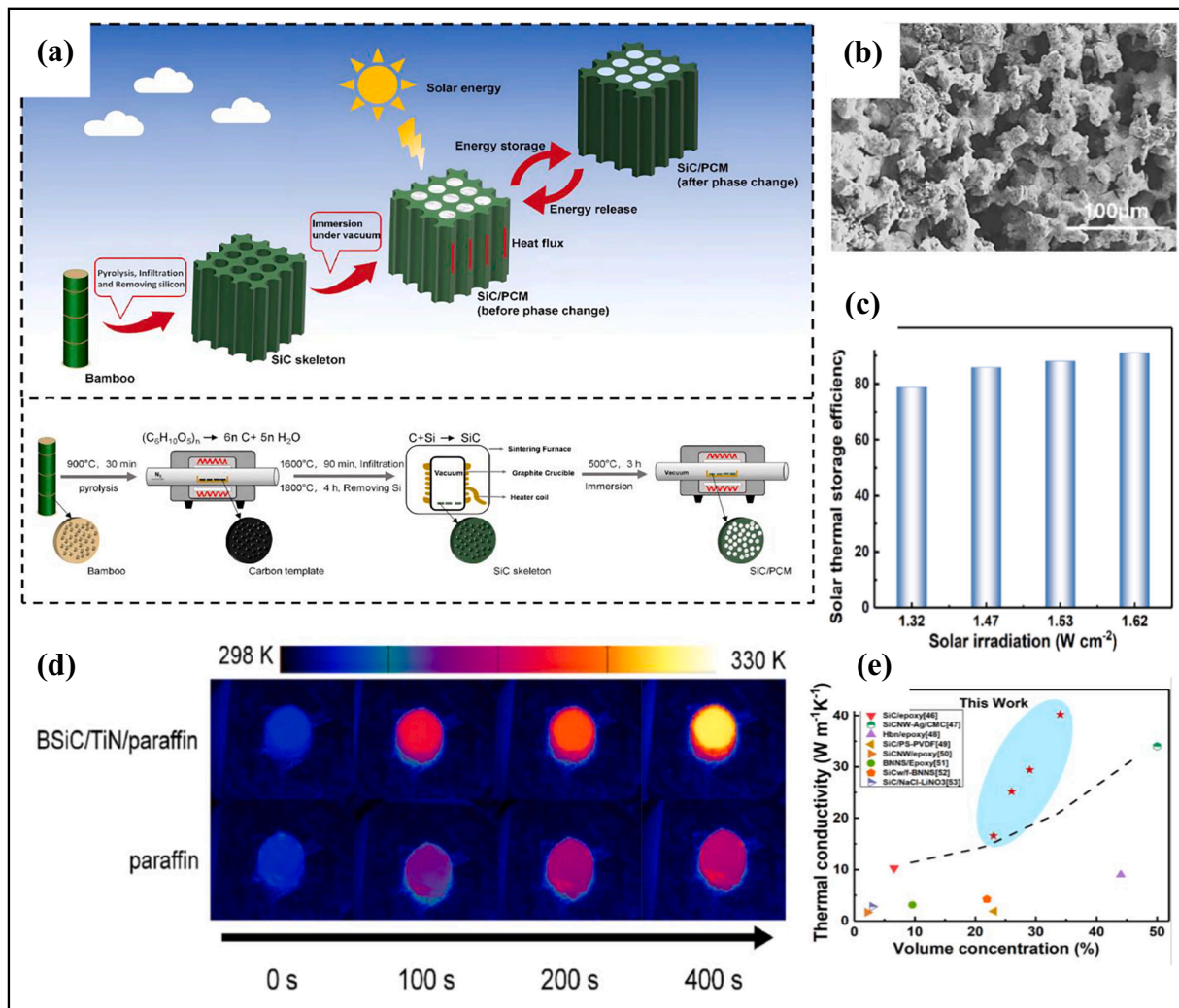It is evident from the study by Hekimoğlu et al. [54] that no

Fig. 11. (a) The concept of solar thermal storage and the method of production of silicon carbide (BSiC) ceramics obtained from bamboo, utilizing phase transition composites, (b) SEM image, (c) Efficacy of BSiC/TiN/paraffin solar thermal storage at different solar irradiation fluxes, (d) Infrared snapshot of paraffin and BSiC/TiN/paraffin under influence solar irradiation, (e) comparison of thermal conductivity between BSiC/paraffin and the several most recent reported ceramic-based composites [61].

distinguishing band evolved during the thermal cycling process when the chemical structures of the WSC/MP and AWSC/MP were contrasted before and after. This outcome is a crucial sign of the materials' strong cycling chemical stability. Based on an observation from a study by Chen et al. [62], PEG peak levels of absorption developed in all of the composite PCMs' spectra when it was fixed into the carbon-based matrixes but no new peaks were noticed. Consequently, no chemical interaction occurred between the PEG molecules and the matrixes, indicating the fact that all of the specimens were suitable substrates for PEG adsorption and that the shape-stable PCMs had good chemical stability in their produced state. The fact that there is no discernible change from the peak observed prior to the 200 cycles afterwards suggests that heat cycling does not have an impact on the PEG crystal arrangement in PEG/400CDF. Following the heat periods, the distinctive peaks in the composite ss-PCMs' Fourier transform infrared (FT-IR) spectrum likewise stay identically, indicating that there is no substance interaction involving the diatom frustules and PEG. Consequently, the PEG/400CDF composite ss-PCMs possess outstanding chemical stability [84]. FR-IR and XRD studies were used to verify the chemical stability of the composite PCM based on the Sheng et al. [87] investigation. These specimens' spectra for the FT-IR and XRD analyses were the same, demonstrating the high consistency of the PW. Additionally, the sisal-

derived carbon at 2400 °C is extremely resilient and has no interaction with PW. Thus, the strong thermal and chemical endurance of both PW and carbon-supporting materials might encourage their ongoing application for TES.

Particularly relevant is the fact that the solubility of BD/BM-CPCMs frequently gets influenced throughout the production technique through the selection of PCM and support substances, in addition towards the impregnation procedure. As brought up prior to that, the support material, commonly a polymer matrix produced from bio-based resources, offers firmness and support, when PCMs are impregnated or immersed inside the supporting structure. The PCMs are inundating or filling the pores in the support material during the impregnation procedure. This preserves the structural qualities of matrices while enabling the hybrid material to take advantage of the PCM's latent potential. On average, because of having intricate and frequently crosslinked architectures, many bio-derived polymers tend to not be very soluble in ordinary solvents. Nonetheless, adding PCMs could have an impact upon the combination of composites PCM's entire solubility. PCMs, whether might be conventional or bio-based oils or waxes, may exhibit particular solvent solubility properties [88].

At elevated temperatures, the whole polymeric 3D cross-linking matrix becomes insoluble and non-fusible. Because of this,
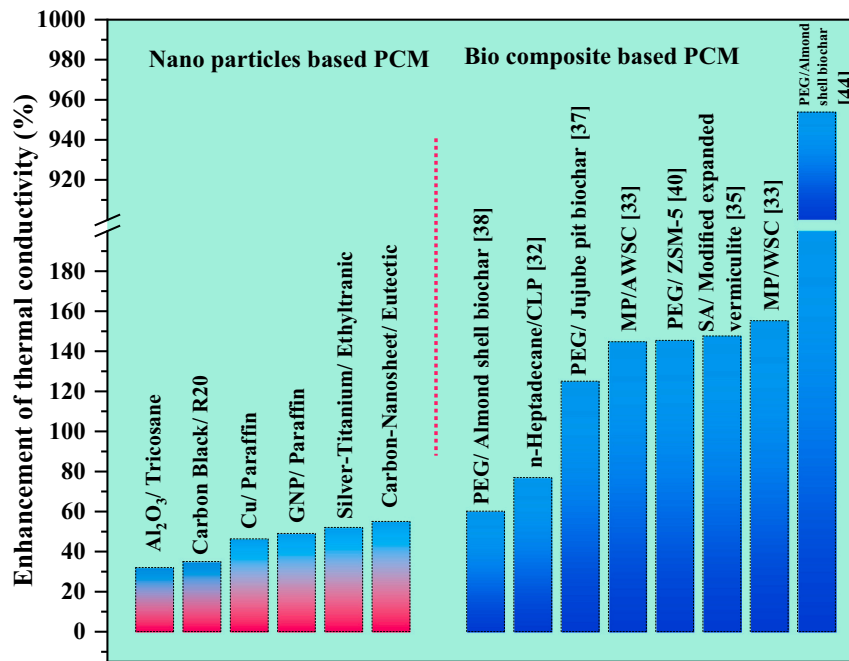
Fig. 12. Thermal conductivity enhancement comparison among various NePCM and bio-based composites.

investigation into the development and manufacturing of polymeric form-stable PCMs (FSPCMs) based on bulk polymers has accelerated recently. Wang et al. [89] suggested encasing paraffin into the polyethylene glycol-polyurethane (PEG-PU) 3D cross-linking structure to produce extremely dependable FSPCMs. The findings demonstrate the exceptional thermal and physical stability of such types of FSPCMs by proving the fact that the 3D network framework can keep the generated FSPCMs from melting even at temperatures above the glass transition temperature of the underlying substances (PEG-PU). Tang et al. produced a pair of dependable FSPCMs with improved enthalpy values (PEG-PU/paraffin [90] and PEG-PU/hexadecanol [91] systems) by modifying the linker enlarging geometry.

3.2.7. Corrosion resistance

Diverse resistance to corrosion qualities is likely exhibited by bio-derived polymers like polylactic acid (PLA) and poly-hydroxyalkanoates (PHA). The particulars and nature of the acidic atmosphere, unfortunately, might influence the level of corrosion resistance in general. Corrosion problems may be caused by PCMs that include salts or certain corrosive agents. The adjacent substances containing suitable PCM are vital in this specific case. Approaches for reducing the deterioration issue with BD/BM-CPCM include encapsulation, modifications to the surface with the addition of nanoparticles, and physical incorporation [92]. Plenty interests have been shown in SiC ceramic honeycomb (SCH), which having open cell pathways and sidewalls featuring good heat conductivity. The excellent thermal conductivity of SCH could be effectively employed as a high-temperature efficient heat exchanger alongside a solar heat collector. Its benefits include an elevated operating temperature, stable thermal behavior, and a relatively low coefficient of expansion upon heating. Most importantly, it resists corrosion when exposed to nitrate salts [93]. Xu et al. [59] noticed that CPCMs continue to show outstanding thermal cycling stability after being exposed to ambient air and going through 1000 perpetual cycles of cooling and heating. Furthermore, following 1000 sessions, there is no longer any chemical connection that exists between paraffin and SiC foam. Furthermore, following cycles, there is no corrosion seen in the CPCM's sample.

3.2.8. Mechanical properties

The impact of the material microencapsulated in bio-sourced polymer shell PCM (m-PCM) on the mechanical properties of the cement mortar was assessed by uniaxial compression testing. The outcomes showed that adding the m-PCM significantly reduced mechanical strength. The strength of compression (CS) kept declining as the m-PCM content increased. The poor inherent strength of the microcapsules and potential damage throughout mortar component integration that could result in PCM leakage in the matrix are most likely to be responsible for the performance degradation. The mean CS of P5 during this stage was 40.39 MPa, away 31.2 % from that of the reference specimen; similarly, the standard deviation of the CS of P10 and P15 was 33.59 MPa and 29.13 MPa, respectively, with a tendency to drop by 42.8 % and 50.4 %, from the benchmark [94].

By integrating LWA loaded with an inexpensive bio-based PCM, composite lightweight aggregates (cLWA) were synthesized and added to a cement mortar to formulate a thermal energy storage concrete (TESC) [95]. Two impregnation techniques and three different types of mineral LWAs—bentonite, sepiolite, and silica gel—were employed. Nevertheless, the TESC utilizing substitution techniques with bentonite and 50 vol% of cLWA never deployed or displayed unsatisfactory mechanical characteristics. The assessments of the CS and the flexural strength for the viable TESC revealed a considerable decrease with the amount of cLWA; however, the flexural strength displayed just a slight decline. Significantly improved outcomes occurred with sepiolite (although decreased by 36 % to 40 %), silica gel, and bentonite trailing behind. The most favorable outcomes were obtained with a substitute of sand throughout the three inclusion strategies. Legal assistance put the lower limit for CS for non-bearing pre-fabricated concrete to roughly 15 MPa in regard to application, notwithstanding more flexible requirements; as a result, sepiolite remained the only alternative left.

4. Enviro-economic aspects of TES: underlying scopes of BD/BM-CPCM

In comparison to fossil fuels, thermal energy storage technologies provide an emission-free, sustainable, and ecologically friendly alternative to energy. They offer a desirable alternative to combat climate change and lessen global warming. These solutions can increase thermal
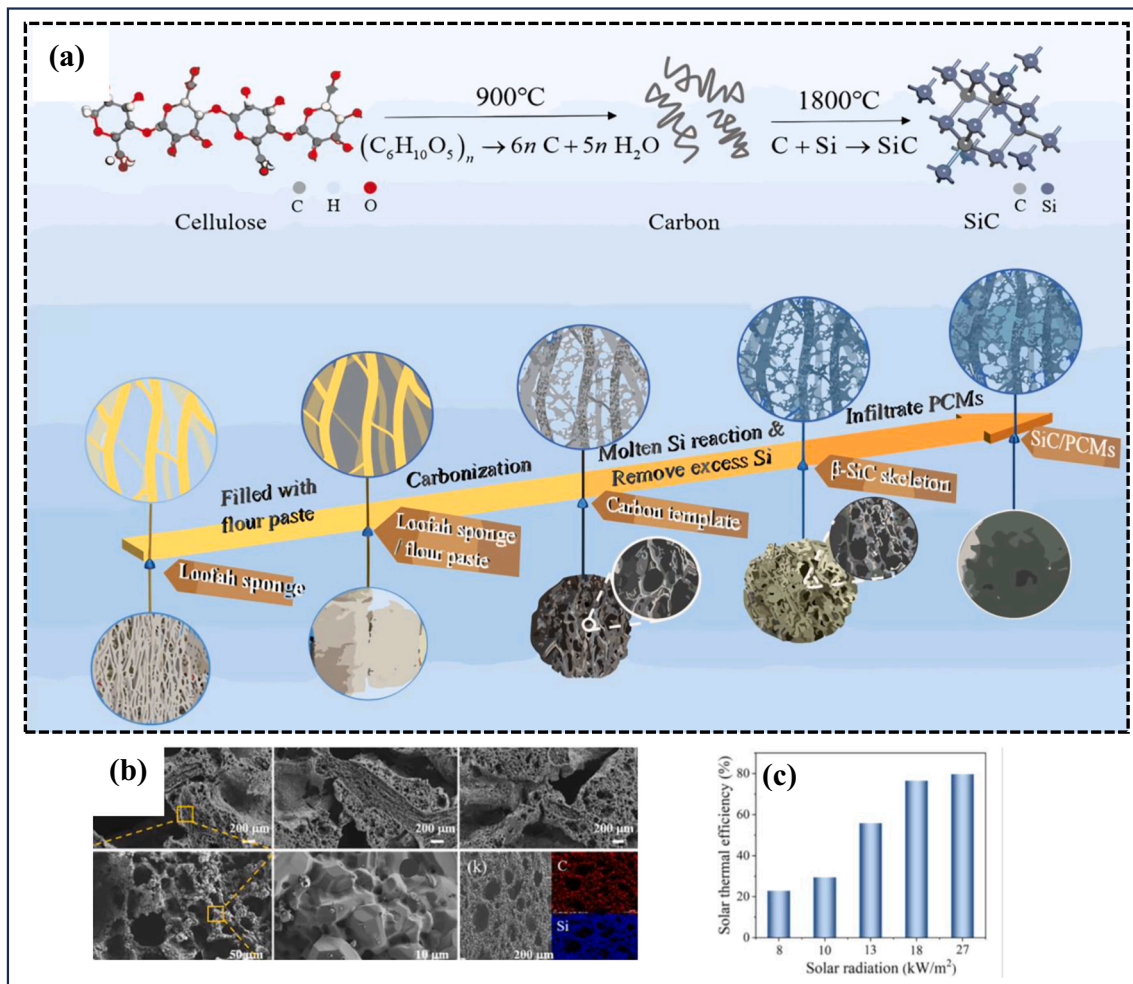
Fig. 13. (a) This technique transforms from loofah to silicon carbide (SiC) and is accompanied by an appropriate molecular structure schematic and an example of the fabrication method for biologically SiC ceramic-based composite phase change materials (CPCMs). The process primarily involves carbonization, molten silicon reaction, eliminating excess silicon, impregnating flour paste to increase the overall strength of loofah sponge, and infiltrating PCMs. The CPCMs that are produced as a result have high heat conductivity, (b) The porousness of the porous biomorphic SiC ceramic decreases to approximately 85 %, 75 %, and 65 % depending on its microstructure. (c) The solar thermal energy efficiency of CPCMs-80 under various sun radiation conditions [59].

efficiency in residential buildings by at least 30 % to 35 % and cut energy use in buildings by up to 50 %, making them an environmentally friendly addition to current systems [96]. PCM-integrated photovoltaic systems release fewer greenhouse emissions than traditional solar heating systems, including CO, SO_2, CO_2, and NO_x. Additionally, these technologies have the potential to reduce carbon emissions by up to 70 % [57]. Sensible heat storage systems can be built and used in building applications with long-term greenhouse gas emissions ranging from 5 to 30 $(gCO_2)_{eq}/kWh_{installed}$. A statistical assessment indicates that the horizontal TES may conserve up to $90,000 annually with a payback period of less than a single year [97].

The capital cost and expenditure for the use of paraffin wax as PCM was covered in another study by He and Setterwall [98] and concluded that adding PCMs as cold storage to already-existing refrigeration systems can double cooling capacity while requiring less additional investment. Additionally, PCM in refrigeration systems can boost operational flexibility and minimize the amount of material needed. A literature review by Gautam et al. [99] found that thermal energy storage proved more cost-effective than either hydrogen storage or lithium-ion batteries. Utilizing thermal energy systems is significantly more cost-effective and practical in renewable energy systems where the investment surpasses $100/MWh. In addition, these systems may deliver energy seven days a week, 24 h a day, without regard to the

quantity of solar radiation present. Because TES systems feature inexpensive storage compartments (less than $ 40/kWh) and lengthy lifespans of at least 20 to 30 years, their use in real-world situations is less expensive overall. If the proper utilization of BD/BM-CPCM with desired thermochemical properties along with suitable charging and discharging rate and heat absorption capability without leakage and corrosion can be implemented, the scenario may drastically change with all the aspects.

One of the significant financial advantages of BD/BM-CPCM is the possibility for energy savings. These innovations can improve thermal storage and heat movement, which raises system efficiency and reduces energy consumption. These technologies can be used to measure energy savings, which can be utilized to figure out the economic benefits of lower energy costs throughout the course of the lifetime of the system. Certain PCMs, such as paraffin wax, are widely utilized, but their lack of improved thermophysical characteristics makes it necessary to enhance their use without raising production costs at a high margin. The utilization of improved permeable carbon reinforces, including graphene or carbon nanotube structure, has significantly improved the composite PCMs' thermal conductivity characteristics. The disadvantages that accompany their widespread use, include extremely expensive and intricate fabrication. However, inexpensive carbon fibers made from sisal will serve as PCMs' thermal stimulating scaffolds, advancing their
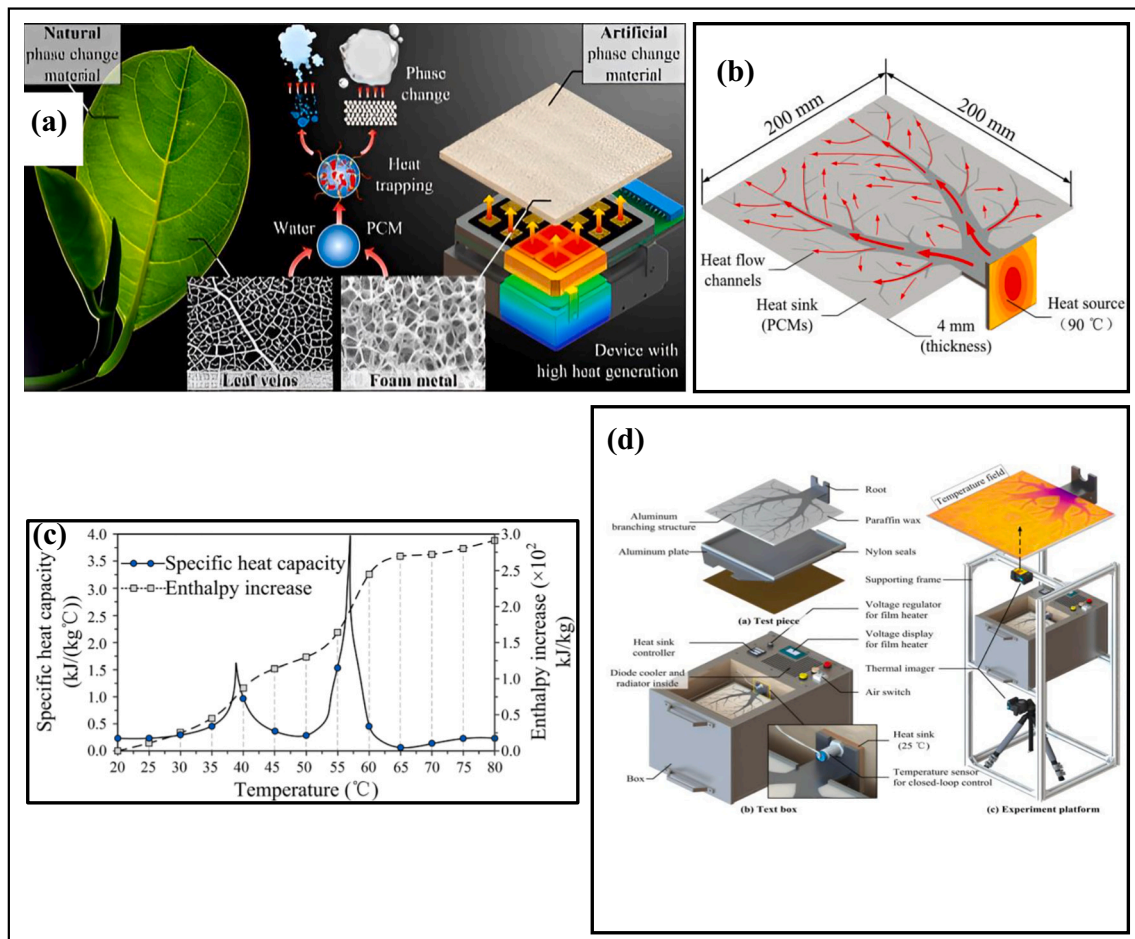
Fig. 14. (a) Comparison of the structure and operation of natural and synthetic PCMs, (b) physical model for heat dispersion, (c) enthalpy rise and specific heat capacity of paraffin wax, (d) platform for experiments [83].

value in capturing solar energy and recyclable heat with less cost [87]. The reduction of the yearly electrical power usage of the greenhouse by approximately 14,577.5 kWh and greenhouses can decrease their annual natural gas usage by a maximum of 1348 kWh by employing bio-means rather than conventional PCM. Moreover, the addition of bio-based PCMs could conserve and lower greenhouse expenses by around 34.4 % to 59 % within the years to come whenever production in large quantities commences [100].

Evaluating the endurance and long-term functionality of BD/BM-CPCM is crucial from an economic perspective. The aforementioned technologies ought to hold their improved properties over time with little maintenance or degeneration. Durable long-term performance ensures that the financial benefits are maintained throughout the solar system. One crucial aspect of economic study is figuring out the return on investment. This means assessing the short- and long-term benefits of BD/BM-CPCM against the upfront costs. Longer lifespans, increased system efficiency, and energy savings should all be prioritized. Positive Return on Investment (ROI) indicates the economic viability and attractiveness of certain technologies.

The scalability and market availability of BD/BM-CPCM impact their economics. When assessing the economic feasibility of these materials, larger-scale availability and cost are important considerations. The economics of such innovations may improve if the production processes are scalable, and the materials are made more generally available. This might result in cost savings and increased adoption. The viability of BD/BM-CPCM depends on the availability of government subsidies, incentives, and policies that favor clean energy technologies. The financial attraction and cost-effectiveness of using these technologies in thermal

energy storage applications could be significantly impacted by these incentives. It is crucial to assess the laws and incentives that exist now and in the future that might promote their use.

5. Heat transfer models during phase change and machine learning scopes for optimization

Studying the situations where phase transition happens is challenging; in fact, locating the solid-liquid boundary in these problems can be challenging because it moves at the rate at which the latent heat of melting is absorbed or released. To address the energy equation, the phase transition problems are investigated analytically, experimentally, and numerically using one, two, or three-dimensional models (Table 3). Researchers that work with PCMs have presented the energy equation in a number of ways. Analyzing several PCM formulations has shown that the enthalpy method formulation is the most often used approach for resolving PCM issues. By eliminating the condition to satisfy in the phase transition zone, the enthalpy technique has the advantage of making the numerical algorithm easier to apply. It was noted that half of the numerical studies that were carried out were two-dimensional.

The results of the numerical approaches that were published show that they were effective in providing solutions for phase transition issues; the majority of these solutions were used to look into and resolve issues in a phase transition. Because phase transition issues might be resolved in the solid state notwithstanding their complexity. But some researchers have made these issues more complicated by include natural convection in the melting zone. Numerical approaches to phase transition problem solving have generally examined the following issues: heat
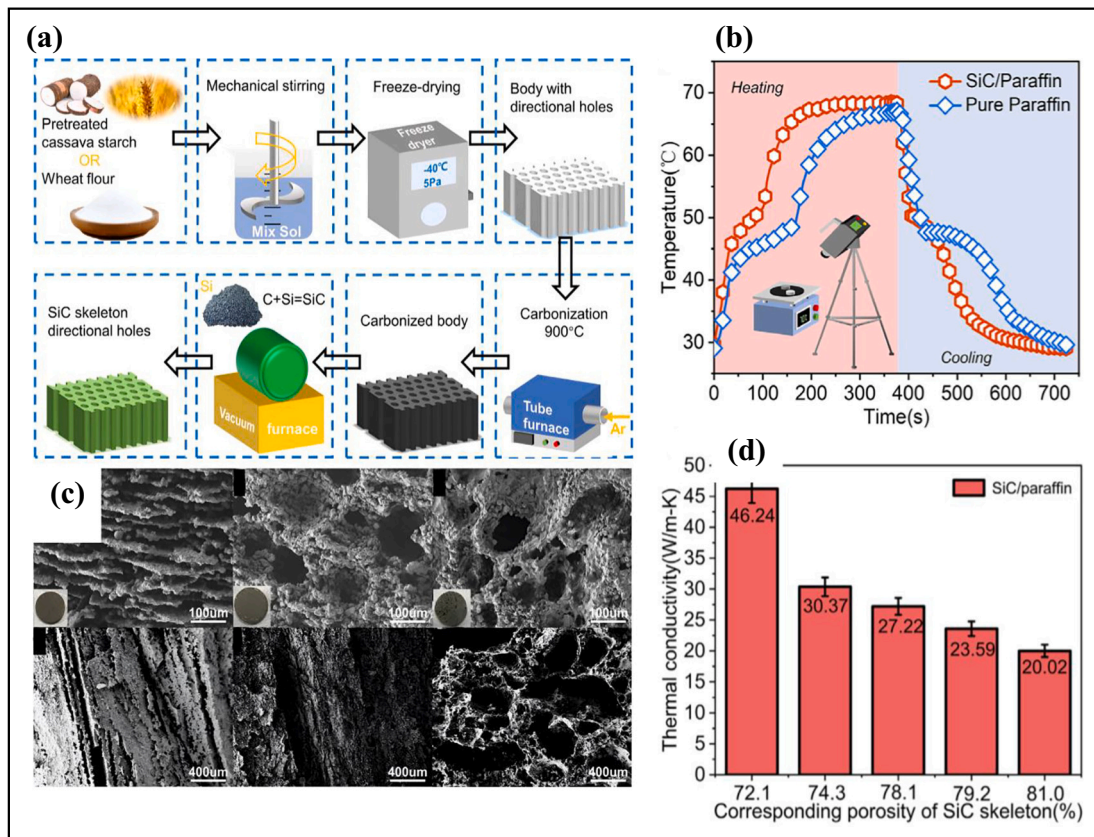
Fig. 15. Procedures for preparation, SEM pictures of (a) porous SiC ceramics, and techniques for making porous SiC ceramics, (b) the temperature profiles corresponding to pure paraffin and SiC/CPCMs, (c) C-SiC, W-SiC, and F-SiC are shown in the upper row's radially cross-section SEM photographs, and C-SiC, W-SiC, and F-SiC are displayed in the bottom row's axially cross-sectional SEM photographs. (d) Thermal conductivity variations of SiC/paraffin CPCMs on the dependency of porosity of the skeleton [66].

transfer via PCM melting or phase transition is examined [101,102]; temperature distribution within PCMs is assessed [103,104]; the melting front and the impact of natural convection in the melting region are identified [105,106]; the entire system's thermal performance and heat capacity are improved [107]; and the charge and discharge rates and the temperature of thermal storage are examined [108,109].

The development of the Adaptive Neuro-Fuzzy Inference System (ANFIS) model aimed to forecast the relative heat flow (mW/mg) characteristics of CPCM (Myristyl alcohol with biochar) specimens. The results demonstrated that the resultant linear membership function and generalized bell-shaped input exhibited the highest degree of suitability for heat flow value prediction. A sensitivity study conducted by ANFIS at the highest phase shift degree throughout the process of modelling revealed a 1.29 % discrepancy between the actual and expected levels of heat flow, with the estimated value being 7.691 mW/mg but the real amount being 7.792 mW/mg [110]. Optimization tests confirmed that applying dragon fruit extract to the nanoparticles shortened the heating and cooling cycle duration by 37 % when contrasted with using PCM and a heat sink regardless of fins for electronic element thermal management [111].

It is advised to carry out research to enhance the performance of bio-derived and bio-mimetic composite PCMs in various industries, as there does not appear any single study focuses on machine learning and optimization for the usage of BD/BM-CPCMs in these fields. Multivariate and multi-objective optimizations, regular design of passive and active systems, and machine learning-based surrogate model generation are of such kind (Fig. 18(a)). Furthermore, thermal performance of BD/BM-CPCMs can be optimized using sophisticated optimization algorithms according to their accuracy and applicability in multivariate and multi-objective optimizations. Thus, the entire optimization process is controlled by the appropriate selection of machine learning algorithms, assessment of research aims, and utilization of relevant variables. Interestingly, it was discovered that exergy analysis requires the application of optimization and machine learning algorithms in order to assess the viability from a technical and financial standpoint as well as the potential effects on the environment or the active system, whether harmful or not. Lastly, as there haven't been many studies done on this subject, it is highly advised that future research concentrate on system design and operational control strategy for BD/BM-CPCMs applications across a range of industries, utilizing cutting-edge machine learning and optimization techniques. To assess technical and financial viability, multiple objective functions are required, including those that look at energy, energy efficiency, simple payback duration, net present value, etc. Each machine learning algorithm's robustness and dependability must be evaluated in light of the intricate heat transfer processes that vary between PCM-using systems. This is because, in terms of feature extraction and algorithm categorizing, every algorithm has distinct benefits of its own (sample algorithm is shown in Fig. 18(b)).

6. Conclusion and future research directions

This review focuses on providing an overview of the features and possible property improvements of combining bio-mimic and bio-derived organic materials with PCMs. Based on the figure-of-merit methodology outlined in this paper, we conclude that BD/BM-CPCM shows extreme improvement on increasing the thermal conductivity in comparison with NePCMs. The increase in adsorption ratio has resulted in a notable improvement in latent heat. When compared to PCM alone, the melting temperature of BD/BM-CPCM tends to drop. Furthermore, using BD/BM-CPCM, thermal energy storage efficiency and capacity
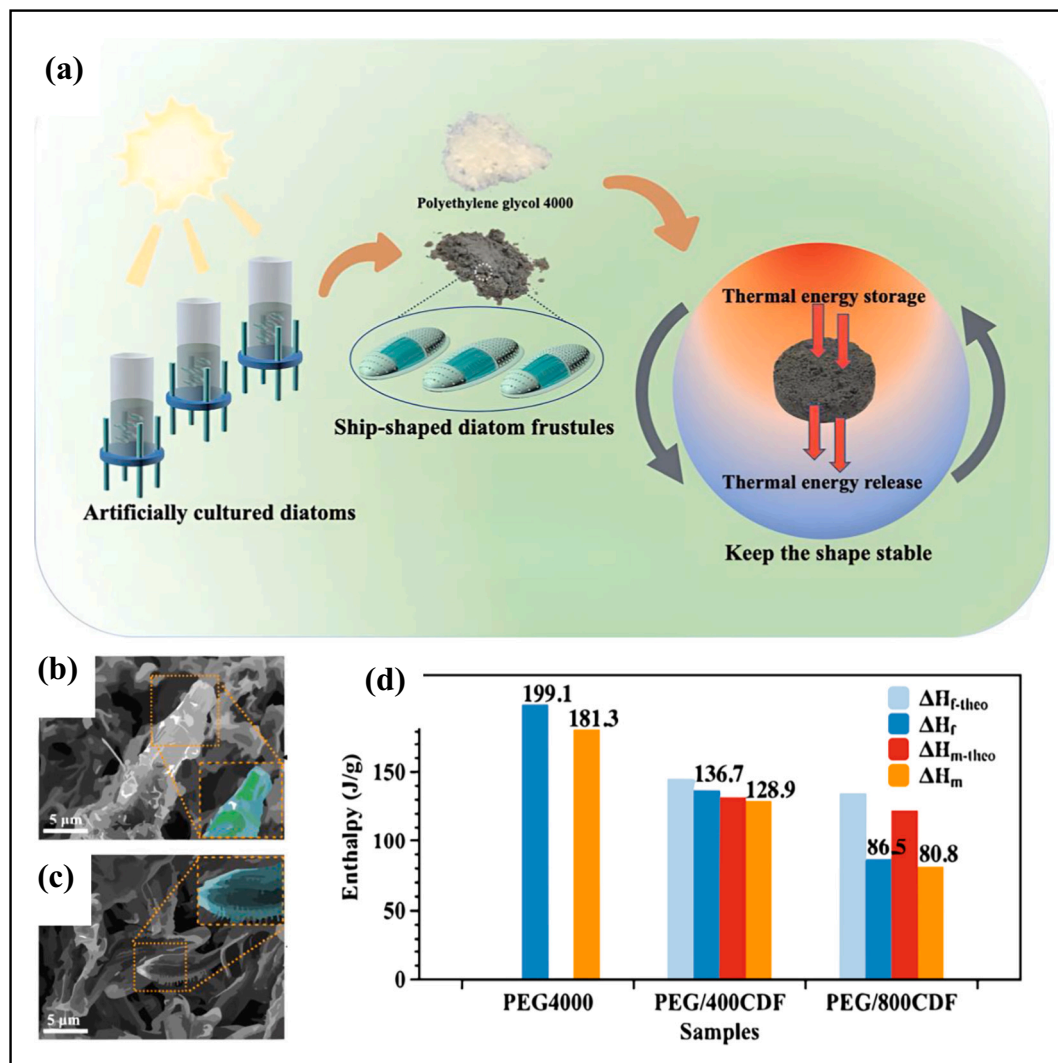
Fig. 16. (a) Diagram showing the steps involved in creating ship-shaped diatom frustules (ss-PCMs) (b) SEM images of the prepared Polyethylene Glycol/400 Calcined diatom frustules(PEG/400CDF), (c) XRD pattern of 400CDF, (d) enthalpy comparison between theoretical and real [84].

increase significantly.

Several studies have observed increases in thermal conductivity of up to 950 % to 1250 %, as well as great thermal stability with no matrix leakage at an average temperature of 150 °C to 250 °C. These types of composites have a relative enthalpy efficiency of up to 98.1 % and can endure 200–1000 heating–cooling cycles on an average. According to the enviro-economic aspects, the proper utilization of BD/BM-CPCM with desired thermochemical properties along with suitable charging and discharging rate and heat absorption capability without leakage and corrosion can be implemented, the scenario may drastically change with all the aspects. The reduction of the yearly electrical power usage of the greenhouse by approximately 14,577.5 kWh and greenhouses can decrease their annual natural gas usage by a maximum of 1348 kWh by employing bio-means rather than conventional PCM. Moreover, the addition of bio-based PCMs could conserve and lower greenhouse expenses by around 34.4 % to 59 % within the years to come whenever production in large quantities commences. To assess technical and financial viability, multiple objective functions are required, including those that look at energy, energy efficiency, simple payback duration, net present value, etc. Each machine learning algorithm's robustness and dependability must be evaluated in light of the intricate heat transfer processes that vary between PCM-using systems.

Although significant effort has been made to enhance the explanatory properties of BD/BM-CPCM and widen the scope of its use in TES systems, there are still significant obstacles to overcome in terms of boosting its latent heat and thermal conductivity and potential efficacy. The recommended correlated future work is listed as follows:

- The heat transfer mechanism inside BD/BM-CPCM is yet unknown because of its complicated composition. More theoretical computations and inventive experimental studies are urgently required to theoretically comprehend the heat flow inside the lump. Limited research has been done on the effects of variables including size, mass fraction, intrinsic thermal conductivity, and formulation of thermally conductive materials on the thermal conductivity of the composite PCM. The aforementioned problems are anticipated to be resolved by fusing sophisticated experiments with cutting-edge machine learning technologies. Even though generating chemical connections between PCM along with matrix and thermally conductive materials has been shown to be a reliable method for increasing thermal conductivity, its manufacturing process needs to be streamlined to make it more cost-competitive.
- More efforts must be made in the future to identify the mechanisms of the confinement effect of biomimetic matrix on the PCM enclosed can both increase thermal stability and decrease latent heat of the composites. In brief, particularly with regard to surface chemistry
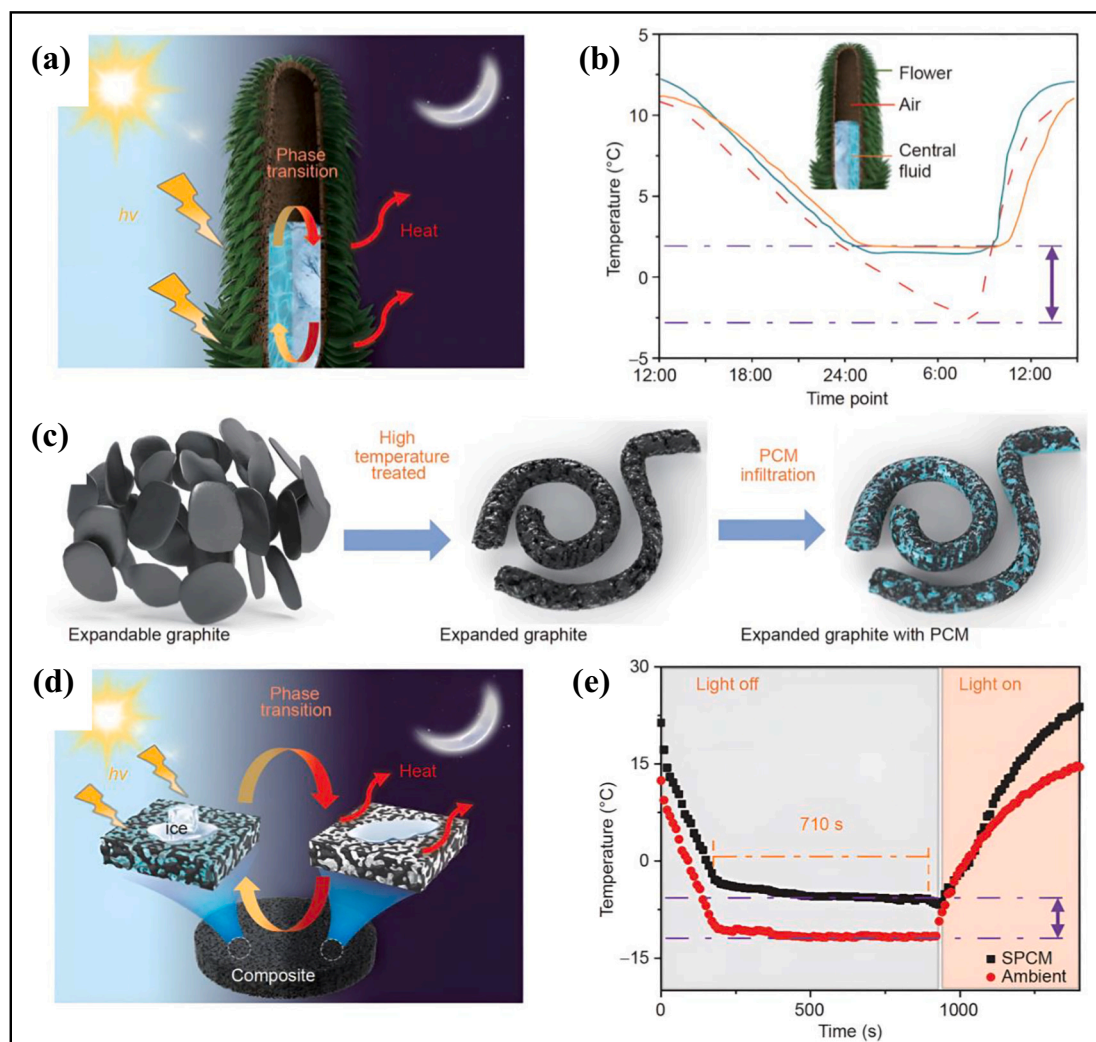
Fig. 17. (a) Diagram illustrating how solar thermal energy is converted and stored in the afro-alpine plant species Lobelia telekii, (b) temperature fluctuations in the plants flower or core fluid and the surrounding air on an average day, (c) diagram demonstrating the production of Expanded Graphite (EG) and a PCM composite for thermal energy storage and solar-thermal conversion, (d) diagram showing the conversion and storage of solar-thermal energy in an solar phase-change material (SPCM), (e) displays the temperature fluctuation of the SPCM exterior at a surrounding temperature of -12 °C under solar radiation (100 m.W/cm^2) [56].

and the most effective polymer modifying agent, in order to further improve the latent heat of composite PCM. Although it has been demonstrated that treating certain nanoparticles with composite in some proportion is a more effective way to improve the thermal properties of PCM in TES, its applicability to other sectors and the corresponding effectiveness still needs to be carefully explored and verified. There are still other methods that can be developed to optimize the crystal transformation in addition to the synthesis procedure.

- With regard to the advancement in substance functionalism, it is necessary to show and research the use of bio-derived composite with innovative effects such as light-thermal conversion, versatility, electro-thermal conversion, and anti-bacterial qualities in real-world systems. Furthermore, since previous studies primarily focused on the production and characterization of lower temperatures in both bio-mimetic and bio-derived composite PCM, it is advised that more emphasis be placed on the development of moderate- and high-temperature PCM composites and their practical application.

- Certain bio-based polymers, such as PLA, PHA and others that are employed as matrices, are susceptible to UV light, which may degrade them and perhaps cause degradation over time. Nevertheless, the result may differ based on the particular matrix and PCM

selection. It is suggested that more focus be given to figuring out how BD/BM-CPCMs behave after being exposed to light, ageing, and the development of bio-based PCM composites with sufficient resistance to degradation.

- It is necessary to design adaptable BD/BM-CPCM for multifunctional energy harvesting and storage. Opportunities for instantaneous energy conversion and retention, made possible by BD/BM-CPCM, have developed recently. It is still challenging to use multifunctional BD/BM-CPCMs widely for effective energy conversion and storage at severe temperatures, even if exceptionally effective energy conversion and storage has been achieved. To improve energy harvesting and raise its efficiency, it is necessary to look into novel approaches to lowering heat loss and improving energy harvesting. Since the efficiency of magnetic-thermal conversion is very low when compared to solar-thermal and electric-thermal conversion efficiencies, more work needs to be done to increase its effectiveness, energy conversion efficiency, and long-term stability in BD/BM-CPCMs.

- It is important to investigate BD/BM-CPCM uses for thermal management. Through the use of apathetic phase transitions, studies on BD/BM-CPCMs-based thermal control primarily aims to prevent the scorching of batteries, building application, structures, or human
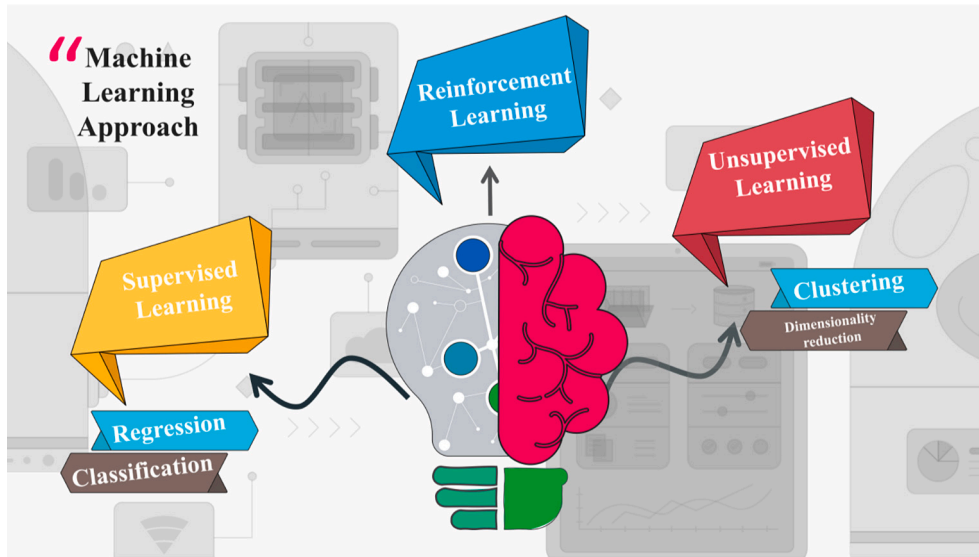
(a)
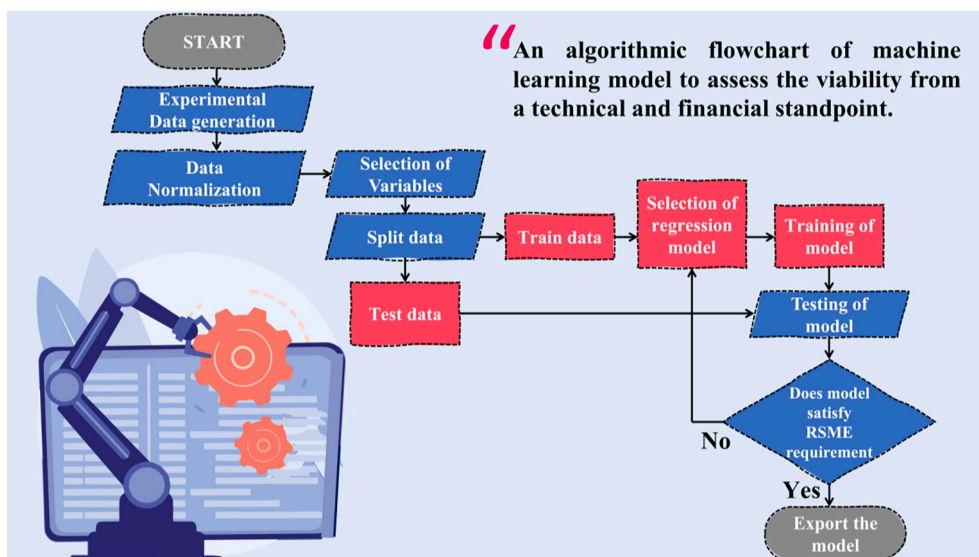
(b)

Fig. 18. (a) Several machine learning approaches in common practice, (b) algorithmic flowchart of machine learning model to assess the viability from a technical and financial standpoint.

Table 3
Heat transfer models to predict the phase transition phenomenon of PCMs.

Remarks	Heat transfer models of phase change problem	Reference
Basic formulation	$\rho\frac{\partial H}{\partial t}=\frac{1}{r}\frac{\partial}{\partial r}\left(kr\frac{\partial T}{\partial r}\right)+\frac{1}{r}\frac{\partial}{\partial \theta}\left(\frac{k}{r}\frac{\partial T}{\partial \theta}\right)$	[112]
Phase change formulation at solid region	$(T\leq T_m-\varepsilon):H=C_pT$	[112]
Phase change formulation at interface	$(T_m-\varepsilon\leq T\leq T_m+\varepsilon):H=C_pT+$ $\left(\frac{\lambda}{2\varepsilon}\right)T-T_m+\varepsilon$	[112]
Phase change formulation at liquid region	$(T\geq T_m+\varepsilon):H=C_pT+\lambda$	[112]
Phase change formulation in cylindrical coordinates for shell and pipe: solid phase of PCM	$\frac{\partial T}{\partial t}+u_0\frac{\partial T}{\partial x}=\alpha_s\frac{\partial^2 T}{\partial x^2}$ $\frac{\partial u}{\partial x}+\frac{\partial v}{\partial y}=0$	[113]
Liquid phase of PCM	$v\frac{\partial^2 v}{\partial x^2}+g\beta(T-T_f)=0$ $\frac{\partial T}{\partial t}+\frac{\partial(uT)}{\partial x}+\frac{\partial(vT)}{\partial y}=\alpha_f\frac{\partial^2 T}{\partial x^2}$	[113]
Phase change formulation in two cylindrical coordinates	$\rho_H C_{p,H}\left(\frac{\partial T_H}{\partial t}+v\frac{\partial T_H}{\partial x}\right)=\frac{4h}{d}(T_p-T_H)+$ $k_H\frac{\partial^2 T_H}{\partial x^2}$ $\frac{\partial H_P}{\partial t}=\frac{1}{r}\frac{\partial}{\partial r}\left(k_p r\frac{\partial T_p}{\partial r}\right)+\frac{\partial}{\partial x}\left(k_p\frac{\partial T_p}{\partial x}\right)$	[114]
	$\frac{\partial H}{\partial t}=\frac{1}{r}\frac{\partial}{\partial r}\left(\alpha r\frac{\partial h}{\partial r}\right)+\frac{\partial}{\partial z}\left(\alpha\frac{\partial h}{\partial z}\right)-\rho\Delta h_f\frac{\partial f}{\partial t}$ $\rho C_p\pi r_i^2\frac{\partial T}{\partial t}=2\pi r_i U(T-T_H)-\dot{m}C_p\frac{\partial T}{\partial z}$	[115]
Phase change relation	$H(T)=h(T)+\rho_s f\Delta h_f$ $h(T)=\int_{t_{bt}}^{t}\rho C_p dT$	[115]
Basic relationships presented for melting and freezing phase change materials	$\frac{\partial T}{\partial t}=\frac{\alpha}{r^w}\frac{\partial}{\partial r}\left(r^w\frac{\partial T}{\partial r}\right)$ For, $r(t)\leq r\leq l, T=T_{cr}, r\leq r(t)$	[116]
	Where, $1+w=\frac{lA}{v}$ with, $w=\begin{cases}0, For\ a\ PCM\ slab\ insulated\ at\ one\ end\\1, For\ a\ PCM\ cylinder\\2, For\ a\ PCM\ sphere\end{cases}$	[116]
Mass conversion equation	$\frac{\partial u_i}{\partial x_i}=0$	[117]
Momentum conversion equation	$\rho\left(\frac{\partial u_i}{\partial t}+u_j\frac{\partial u_i}{\partial x_j}\right)=\frac{\partial\sigma_{ij}}{\partial x_j}-\rho g\beta(T-T_{ref})\frac{\partial x_2}{\partial x_i}$ $\partial\sigma_{ij}=-p\delta_{ij}-\mu\left(\frac{\partial u_i}{\partial x_j}+\frac{\partial u_j}{\partial x_i}\right)$ $p=p^{'}+\rho gx_2$	[117]
Energy conversion equation	$\rho C_p\left(\frac{\partial T}{\partial t}+u_j\frac{\partial T}{\partial x_j}\right)=\frac{\partial}{\partial x_i}\left(k\frac{\partial T}{\partial x_j}\right)$	[117]

body. Even though the development of high-performance BD/BM-CPCMs with higher quantities of energy storage and thermal conductivity can further enhance the thermal management performance of BD/BM-CPCMs, more attention should be paid in the future to the integration of active thermal management and BD/BM-CPCM-based passive thermal management for both cooling and heating demands.

CRediT authorship contribution statement

Md. Shahriar Mohtasim: Writing – review & editing, Writing – original draft, Methodology, Investigation, Formal analysis, Conceptualization. **Barun K. Das:** Writing – review & editing, Supervision, Formal analysis, Conceptualization.

Declaration of competing interest

The authors declare that they have no known competing financial interests or personal relationships that could have appeared to influence

the work reported in this paper.

Data availability

No data was used for the research described in the article.

References

[1] D. Roy, R. Hassan, B.K. Das, A hybrid renewable-based solution to electricity and freshwater problems in the off-grid Sundarbans region of India: optimum sizing and socio-enviro-economic evaluation, J. Clean. Prod. 372 (2022) 133761.

[2] J. Goodenough, Energy storage materials: a perspective, Energy Storage Mater. 1 (2015) (2020) 158–161.

[3] S.W. Sharshir, et al., Thermal energy storage using phase change materials in building applications: a review of the recent development, Energ. Buildings. 285 (2023) 112908.

[4] X. Man, et al., Review on the thermal property enhancement of inorganic salt hydrate phase change materials, Journal of Energy Storage 72 (2023) 108699.

[5] M. Sun, et al., A review on thermal energy storage with eutectic phase change materials: fundamentals and applications, Journal of Energy Storage 68 (2023) 107713.

[6] M. Mehling, L.F. Cabeza, Phase change materials and their basic properties, in: Thermal Energy Storage for Sustainable Energy Consumption: Fundamentals, Case Studies and Design, Springer, 2007, pp. 257–277.

[7] M. Kenisarin, K. Mahkamov, Solar energy storage using phase change materials, Renew. Sustain. Energy Rev. 11 (9) (2007) 1913–1965.

[8] P. Pardo, et al., A review on high temperature thermochemical heat energy storage, Renew. Sustain. Energy Rev. 32 (2014) 591–610.

[9] A. Joulin, et al., Experimental and numerical investigation of a phase change material: thermal-energy storage and release, Appl. Energy 88 (7) (2011) 2454–2462.

[10] M. Medrano, et al., Experimental evaluation of commercial heat exchangers for use as PCM thermal storage systems, Appl. Energy 86 (10) (2009) 2047–2055.

[11] L. Prasad, P. Muthukumar, Design and optimization of lab-scale sensible heat storage prototype for solar thermal power plant application, Solar Energy 97 (2013) 217–229.

[12] H. Niyas, C.R.C. Rao, P. Muthukumar, Performance investigation of a lab-scale latent heat storage prototype–experimental results, Solar Energy 155 (2017) 971–984.

[13] S. Tuly, et al., Investigating the energetic, exergetic, and sustainability aspects of a solar still integrating fins, wick, phase change materials, and external condenser, Journal of Energy Storage 55 (2022) 105462.

[14] X. Wang, et al., A critical review on phase change materials (PCM) for sustainable and energy efficient building: design, characteristic, performance and application, Energ. Buildings 260 (2022) 111923.

[15] B. Xu, P. Li, C. Chan, Application of phase change materials for thermal energy storage in concentrated solar power plants: a review to recent developments, Appl. Energy 160 (2015) 286–307.

[16] B. Fumey, R. Weber, L. Baldini, Heat transfer constraints and performance mapping of a closed liquid sorption heat storage process, Appl. Energy 335 (2023) 120755.

[17] B.K. Choure, T. Alam, R. Kumar, A review on heat transfer enhancement techniques for PCM based thermal energy storage system, Journal of Energy Storage 72 (2023) 108161.

[18] C.N. Elias, V.N. Stathopoulos, A comprehensive review of recent advances in materials aspects of phase change materials in thermal energy storage, Energy Procedia 161 (2019) 385–394.

[19] C. Suresh, R.P. Saini, Thermal performance of sensible and latent heat thermal energy storage systems, International Journal of Energy Research 44 (6) (2020) 4743–4758.

[20] D. Gielen, et al., The role of renewable energy in the global energy transformation, Energ. Strat. Rev. 24 (2019) 38–50.

[21] R. Hassan, B.K. Das, M. Hasan, Integrated off-grid hybrid renewable energy system optimization based on economic, environmental, and social indicators for sustainable development, Energy 250 (2022) 123823.

[22] P. Zhang, X. Xiao, Z. Ma, A review of the composite phase change materials: fabrication, characterization, mathematical modeling and application to performance enhancement, Appl. Energy 165 (2016) 472–510.

[23] L. Lv, et al., Experimental study of screening polyols and their binary eutectic phase change materials for long-term thermal energy storage, J. Clean. Prod. 399 (2023) 136636.

[24] S. Tuly, et al., Performance investigation of active double slope solar stills incorporating internal sidewall reflector, hollow circular fins, and nanoparticle-mixed phase change material, Journal of Energy Storage 55 (2022) 105660.

[25] N. Zhang, et al., Latent heat thermal energy storage systems with solid–liquid phase change materials: a review, Adv. Eng. Mater. 20 (6) (2018) 1700753.

[26] X. Guo, J. Feng, Facilely prepare passive thermal management materials by foaming phase change materials to achieve long-duration thermal insulation performance, Compos. Part B Eng. 245 (2022) 110203.

[27] Y. Cao, et al., Multifunctional phase change composites based on biomass/MXene-derived hybrid scaffolds for excellent electromagnetic interference shielding and superior solar/electro-thermal energy storage, Nano Res. 15 (9) (2022) 8524–8535.

[28] J. Xu, et al., Synergizing piezoelectric and plasmonic modulation of Ag/BiFeO3 fibrous heterostructure toward boosted photoelectrochemical energy conversion, Nano Energy 89 (2021) 106317.

[29] S. Tuly, et al., Investigation of a modified double slope solar still integrated with nanoparticle-mixed phase change materials: energy, exergy, exergo-economic, environmental, and sustainability analyses, Case Studies in Thermal Engineering 37 (2022) 102256.

[30] M. Du, et al., Bio-composite bacterial cellulose/melamine foam to prepare advanced phase change materials with sandwich structures for thermal storage and energy conversion, Journal of Energy Storage 66 (2023) 107381.

[31] A.A. Mehrizi, et al., Application of bio-based phase change materials for effective heat management, Journal of Energy Storage 61 (2023) 106859.

[32] M. Nazari, M. Jebrane, N. Terziev, New hybrid bio-composite based on epoxidized linseed oil and wood particles hosting ethyl palmitate for energy storage in buildings, Energy 278 (2023) 127692.

[33] T. Li, et al., High energy-density and power-density thermal storage prototype with hydrated salt for hot water and space heating, Appl. Energy 248 (2019) 406–414.

[34] M.G. Kibria, et al., Impact of hybrid nano PCM (paraffin wax with Al2O3 and ZnO nanoparticles) on photovoltaic thermal system: energy, exergy, exergoeconomic and enviroeconomic analysis, J. Clean. Prod. 436 (2024) 140577.

[35] B. Kalidasan, et al., Phase change materials integrated solar thermal energy systems: global trends and current practices in experimental approaches, Journal of Energy Storage 27 (2020) 101118.

[36] N. Kumar, et al., Review of stability and thermal conductivity enhancements for salt hydrates, Journal of Energy Storage 24 (2019) 100794.

[37] A. Venugopal, et al., Nano-enhanced phase change material for thermal comfort at skull and environment interface in riding helmets: an experimental investigation, Journal of Energy Storage 50 (2022) 104332.

[38] A. Dwivedi, A. Kumar, V. Goel, A consolidated decision-making framework for nano-additives selection in battery thermal management applications, Journal of Energy Storage 59 (2023) 106565.

[39] J.M. Mahdi, et al., Intensifying the thermal response of PCM via fin-assisted foam strips in the shell-and-tube heat storage system, Journal of Energy Storage 45 (2022) 103733.

[40] Z.-R. Li, N. Hu, L.-W. Fan, Nanocomposite phase change materials for high-performance thermal energy storage: a critical review, Energy Storage Materials 55 (2023) 727–753.

[41] B. Kalidasan, et al., Green synthesized 3D coconut shell biochar/polyethylene glycol composite as thermal energy storage material, Sustain Energy Technol Assess 60 (2023) 103505.

[42] X. Yue, et al., Bamboo-derived phase change material with hierarchical structure for thermal energy storage of building, Journal of Energy Storage 62 (2023) 106911.

[43] H. Gao, et al., Ambient pressure dried flexible silica aerogel for construction of monolithic shape-stabilized phase change materials, Solar Energy Materials and Solar Cells 201 (2019) 110122.

[44] C. Cárdenas-Ramírez, F. Jaramillo, M. Gómez, Systematic review of encapsulation and shape-stabilization of phase change materials, Journal of Energy Storage 30 (2020) 101495.

[45] W. Liu, et al., Heat transfer enhancement of latent heat thermal energy storage in solar heating system: a state-of-the-art review, Journal of Energy Storage 46 (2022) 103727.

[46] A. Jain, M. Parhizi, Theoretical analysis of phase change heat transfer and energy storage in a spherical phase change material with encapsulation, International Journal of Heat and Mass Transfer 185 (2022) 122348.

[47] T. Li, et al., Experimental investigation on copper foam/hydrated salt composite phase change material for thermal energy storage, International Journal of Heat and Mass Transfer 115 (2017) 148–157.

[48] X. Hu, F. Zhu, X. Gong, Experimental and numerical study on the thermal behavior of phase change material infiltrated in low porosity metal foam, Journal of Energy Storage 26 (2019) 101005.

[49] X. Zhang, et al., Shape-stabilized composite phase change materials with high thermal conductivity based on stearic acid and modified expanded vermiculite, Renew. Energy 112 (2017) 113–123.

[50] D. Das, et al., A novel form stable PCM based bio composite material for solar thermal energy storage applications, Journal of Energy Storage 30 (2020) 101403.

[51] G. Hekimoğlu, et al., Porous biochar/heptadecane composite phase change material with leak-proof, high thermal energy storage capacity and enhanced thermal conductivity, Powder Technol. 394 (2021) 1017–1025.

[52] Y. Lin, et al., Spider web-inspired graphene skeleton-based high thermal conductivity phase change nanocomposites for battery thermal management, Nano-Micro Letters 13 (1) (2021) 180.

[53] T. Chen, et al., Fatty amines/graphene sponge form-stable phase change material composites with exceptionally high loading rates and energy density for thermal energy storage, Chem. Eng. J. 382 (2020) 122831.

[54] D. Liu, et al., A multidirectionally thermoconductive phase change material enables high and durable electricity via real-environment solar–thermal–electric conversion, ACS Nano 14 (11) (2020) 15738–15747.

[55] S. Palanti, et al., Bio-based phase change materials for wooden building applications, Forests 13 (4) (2022) 603.

[56] S. Sheng, et al., Bioinspired solar anti-icing/de-icing surfaces based on phase-change materials, Science China-Materials 65 (5) (2022) 1369–1376.

[57] S.K. Pathak, et al., Energy, exergy, economic and environmental analyses of solar air heating systems with and without thermal energy storage for sustainable development: a systematic review, Journal of Energy Storage 59 (2023) 106521.

[58] Y. Chang, et al., Review on ceramic-based composite phase change materials: preparation, characterization and application, Composites Part B: Engineering 254 (2023) 110584.

[59] Q. Xu, et al., Loofah-derived eco-friendly SiC ceramics for high-performance sunlight capture, thermal transport, and energy storage, Energy Storage Materials 45 (2022) 786–795.

[60] W. Zhang, et al., Lauric-stearic acid eutectic mixture/carbonized biomass waste corn cob composite phase change materials: preparation and thermal characterization, Thermochim. Acta 674 (2019) 21–27.

[61] X. Liu, et al., Bamboo derived SiC ceramics-phase change composites for efficient, rapid, and compact solar thermal energy storage, Solar Energy Materials and Solar Cells 240 (2022) 111726.

[62] Y. Chen, et al., A novel strategy for enhancing the thermal conductivity of shape-stable phase change materials via carbon-based in situ reduction of metal ions, J. Clean. Prod. 243 (2020) 118627.

[63] C. Li, et al., Synthesis and characterization of PEG/ZSM-5 composite phase change materials for latent heat storage, Renew. Energy 121 (2018) 45–52.

[64] R. Wen, et al., Preparation and thermal properties of fatty acid/diatomite form-stable composite phase change material for thermal energy storage, Solar Energy Materials and Solar Cells 178 (2018) 273–279.

[65] J. Liang, et al., Fabrication and characterization of fatty acid/wood-flour composites as novel form-stable phase change materials for thermal energy storage, Energ. Buildings 171 (2018) 88–99.

[66] Y. Song, et al., High-performance thermal energy storage and thermal management via starch-derived porous ceramics-based phase change devices, International Journal of Heat and Mass Transfer 197 (2022) 123337.

[67] Y.-c. Wan, et al., A promising form-stable phase change material prepared using cost effective pinecone biochar as the matrix of palmitic acid for thermal energy storage, Sci. Rep. 9 (1) (2019) 11535.

[68] X. Liu, et al., Nacre-like ceramics-based phase change composites for concurrent efficient solar-to-thermal conversion and rapid energy storage, Solar Energy Materials and Solar Cells 230 (2021) 111240.

[69] Y. Zhao, et al., Honeycomb-like structured biological porous carbon encapsulating PEG: a shape-stable phase change material with enhanced thermal conductivity for thermal energy storage, Energ. Buildings 158 (2018) 1049–1062.

[70] Y. He, et al., Bio-based flexible phase change composite film with high thermal conductivity for thermal energy storage, Compos. A: Appl. Sci. Manuf. 151 (2021) 106638.

[71] A. Balaji, et al., Investigation of thermal energy storage (TES) with lotus stem biocomposite block using PCM, Cleaner Engineering and Technology 4 (2021) 100146.

[72] X. Sheng, et al., MXene-wrapped bio-based pomelo peel foam/polyethylene glycol composite phase change material with enhanced light-to-thermal conversion efficiency, thermal energy storage capability and thermal conductivity, Compos. A: Appl. Sci. Manuf. 138 (2020) 106067.

[73] X. Hu, et al., Novel bio-based composite phase change materials with reduced graphene oxide-functionalized spent coffee grounds for efficient solar-to-thermal energy storage, Solar Energy Materials and Solar Cells 219 (2021) 110790.

[74] G. Hekimoğlu, et al., Walnut shell derived bio-carbon/methyl palmitate as novel composite phase change material with enhanced thermal energy storage properties, Journal of Energy Storage 35 (2021) 102288.

[75] S. Liu, et al., Shape-stable composite phase change materials encapsulated by bio-based balsa wood for thermal energy storage, Solar Energy Materials and Solar Cells 230 (2021) 111187.

[76] X. Lu, et al., A novel bio-based polyurethane/wood powder composite as shape-stable phase change material with high relative enthalpy efficiency for solar thermal energy storage, Solar Energy Materials and Solar Cells 200 (2019) 109987.

[77] Y. Dong, et al., Thermal performance analysis of PCM capsules packed-bed system with biomimetic leaf hierarchical porous structure, J. Therm. Sci. 30 (2021) 1559–1571.

[78] J. Gao, et al., Facile functionalized mesoporous silica using biomimetic method as new matrix for preparation of shape-stabilized phase-change material with improved enthalpy, Int. J. Energy Res. 43 (14) (2019) 8649–8659.

[79] C. Liu, et al., Knitting aryl network polymers (KAPs)-embedded copper foam enables highly efficient thermal energy storage, J. Mater. Chem. A 8 (30) (2020) 15177–15186.

[80] J. Gao, et al., Shape-stabilized phase change material with enhanced thermal conductivity fabricated based on biomimetic polymerization and in situ reduction of Cu ions, International Journal of Energy Research 45 (2) (2021) 2058–2069.

[81] L. Qiu, et al., Bionic hierarchical porous aluminum nitride ceramic composite phase change material with excellent heat transfer and storage performance, Composites Communications 27 (2021) 100892.

[82] B. Xie, W.-l. Cheng, Z.-m. Xu, Studies on the effect of shape-stabilized PCM filled aluminum honeycomb composite material on thermal control, International Journal of Heat and Mass Transfer 91 (2015) 135–143.

[83] H. Liu, et al., Optimizing heat-absorption efficiency of phase change materials by mimicking leaf vein morphology, Appl. Energy 269 (2020) 114982.

[84] B. Wu, et al., Biomass-based shape-stabilized phase change materials from artificially cultured ship-shaped diatom frustules with high enthalpy for thermal energy storage, Compos. Part B Eng. 205 (2021) 108500.

[85] Y. Liang, et al., Sponge gourd-bioinspired phase change material with high thermal conductivity and excellent shape-stability, Journal of Energy Storage 39 (2021) 102634.

[86] J. Huang, et al., Improving the thermal energy storage capability of diatom-based biomass/polyethylene glycol composites phase change materials by artificial culture methods, Solar Energy Materials and Solar Cells 219 (2021) 110797.

[87] N. Sheng, et al., Honeycomb carbon fibers strengthened composite phase change materials for superior thermal energy storage, Appl. Therm. Eng. 164 (2020) 114493.

[88] R. Naresh, R. Parameshwaran, V.V. Ram, Bio-based phase-change materials, in: Bio-Based Materials and Biotechnologies for Eco-Efficient Construction, Elsevier, 2020, pp. 203–242.

[89] K. Chen, et al., Preparation and characterization of form-stable paraffin/ polyurethane composites as phase change materials for thermal energy storage, Energ. Conver. Manage. 77 (2014) 13–21.

[90] Y. Zhang, et al., Form-stable phase change materials with high phase change enthalpy from the composite of paraffin and cross-linking phase change structure, Appl. Energy 184 (2016) 241–246.

[91] B. Tang, et al., Hexadecanol/phase change polyurethane composite as form-stable phase change material for thermal energy storage, Sol. Energy Mater. Sol. Cells 144 (2016) 1–6.

[92] A. Yadav, et al., A systematic review on bio-based phase change materials, International Journal of Automotive and Mechanical Engineering 20 (2) (2023) 10547–10558.

[93] Y. Li, et al., Characterization and thermal performance of nitrate mixture/SiC ceramic honeycomb composite phase change materials for thermal energy storage, Appl. Therm. Eng. 81 (2015) 193–197.

[94] X. Jin, et al., Development of nanomodified eco-friendly thermal energy storing cementitious composite using PCM microencapsulated in biosourced encapsulation shell, Case Studies in Construction Materials 19 (2023) e02447.

[95] E. Franquet, N. Lamrous, Mechanical and thermal characterizations of various thermal energy storage concretes including low-cost bio-sourced PCM, Energ. Buildings 241 (2021) 110878.

[96] I. Dincer, M.A. Rosen, Energetic, environmental and economic aspects of thermal energy storage systems for cooling capacity, Appl. Therm. Eng. 21 (11) (2001) 1105–1117.

[97] S. Thaker, et al., Evaluating energy and greenhouse gas emission footprints of thermal energy storage systems for concentrated solar power applications, Journal of Energy Storage 26 (2019) 100992.

[98] B. He, F. Setterwall, Technical grade paraffin waxes as phase change materials for cool thermal storage and cool storage systems capital cost estimation, Energ. Conver. Manage. 43 (13) (2002) 1709–1723.

[99] K.R. Gautam, G.B. Andresen, M. Victoria, Review and techno-economic analysis of emerging thermo-mechanical energy storage technologies, Energies 15 (17) (2022) 6328.

[100] M.H. Jahangir, M. Ziyaei, A. Kargarzadeh, Evaluation of thermal behavior and life cycle cost analysis of greenhouses with bio-phase change materials in multiple locations, Journal of Energy Storage 54 (2022) 105176.

[101] B. Gürel, A numerical investigation of the melting heat transfer characteristics of phase change materials in different plate heat exchanger (latent heat thermal energy storage) systems, International Journal of Heat and Mass Transfer 148 (2020) 119117.

[102] M. Aadmi, M. Karkri, M. El Hammouti, Heat transfer characteristics of thermal energy storage for PCM (phase change material) melting in horizontal tube: numerical and experimental investigations, Energy 85 (2015) 339–352.

[103] F. Goia, M. Perino, M. Haase, A numerical model to evaluate the thermal behaviour of PCM glazing system configurations, Energ. Buildings 54 (2012) 141–153.

[104] P. Dolado, et al., Characterization of melting and solidification in a real scale PCM-air heat exchanger: numerical model and experimental validation, Energ. Conver. Manage. 52 (4) (2011) 1890–1907.

[105] S. Wang, A. Faghri, T.L. Bergman, A comprehensive numerical model for melting with natural convection, Int. J. Heat Mass Transf. 53 (9–10) (2010) 1986–2000.

[106] O. Bertrand, et al., Melting driven by natural convection a comparison exercise: first results, Int. J. Therm. Sci. 38 (1) (1999) 5–26.

[107] Y. Fang, J. Niu, S. Deng, Numerical analysis for maximizing effective energy storage capacity of thermal energy storage systems by enhancing heat transfer in PCM, Energ. Buildings 160 (2018) 10–18.

[108] S. Bellan, et al., Numerical analysis of charging and discharging performance of a thermal energy storage system with encapsulated phase change material, Appl. Therm. Eng. 71 (1) (2014) 481–500.

[109] W.-W. Wang, et al., Numerical study of the heat charging and discharging characteristics of a shell-and-tube phase change heat storage unit, Appl. Therm. Eng. 58 (1–2) (2013) 542–553.

[110] M. Goud, F. Raval, A sustainable biochar-based shape stable composite phase change material for thermal management of a lithium-ion battery system and hybrid neural network modeling for heat flow prediction, Journal of Energy Storage 56 (2022) 106163.

[111] M. Arulprakasajothi, et al., Optimizing heat transfer efficiency in electronic component cooling through fruit waste-derived phase change material, Journal of Energy Storage 80 (2024) 110238.

[112] R. Velraj, et al., Experimental analysis and numerical modelling of inward solidification on a finned vertical tube for a latent heat storage unit, Sol. Energy 60 (5) (1997) 281–290.

[113] Z. Zongqin, A. Bejan, The problem of time-dependent natural convection melting with conduction in the solid, Int. J. Heat Mass Transf. 32 (12) (1989) 2447–2457.

[114] Z.-X. Gong, A.S. Mujumdar, Finite-element analysis of cyclic heat transfer in a shell-and-tube latent heat energy storage exchanger, Appl. Therm. Eng. 17 (6) (1997) 583–591.

[115] M. Lacroix, Numerical simulation of a shell-and-tube latent heat thermal energy storage unit, Sol. Energy 50 (4) (1993) 357–367.

[116] A. Solomon, Melt time and heat flux for a simple PCM body, Solar Energy 22 (3) (1979) 251–257.

[117] H. Inaba, C. Dai, A. Horibe, Natural convection heat transfer of microemulsion phase-change-material slurry in rectangular cavities heated from below and cooled from above, Int. J. Heat Mass Transf. 46 (23) (2003) 4427–4438.